Edinburgh Research Explorer

Weakly coupled heat bath models for Gibbs-like invariant states in nonlinear wave equations

Weakly coupled heat bath models for Gibbs-like invariant states in nonlinear wave equations

J Bajars[1], J E Frank[1] and B J Leimkuhler[2]

[1] Centrum Wiskunde & Informatica, P.O. Box 94079, 1090 GB Amsterdam, the Netherlands

E-mail: `jason@cwi.nl`

[2] School of Mathematics and Maxwell Institute for Mathematical Sciences, The University of Edinburgh, James Clerk Maxwell Building, The Kings Buildings, Mayfield Road, Edinburgh, Scotland EH9 3JZ

E-mail: `b.leimkuhler@ed.ac.uk`

Abstract. Thermal bath coupling mechanisms as utilized in molecular dynamics are applied to partial differential equation models. Working from a semi-discrete (Fourier mode) formulation for the Burgers or KdV equation, we introduce auxiliary variables and stochastic perturbations in order to drive the system to sample a target ensemble which may be a Gibbs state or, more generally, any smooth distribution defined on a constraint manifold. We examine the ergodicity of approaches based on coupling of the heat bath to the high wave numbers, with the goal of controlling the ensemble through the fast modes. We also examine different thermostat methods in the extent to which dynamical properties are corrupted in order to accurately compute the average of a desired observable with respect to the invariant distribution. The principal observation of this paper is that convergence to the invariant distribution can be achieved by thermostatting just the highest wave number, while the evolution of the slowest modes is little affected by such a thermostat.

AMS classification scheme numbers: 82B99, 65P10, 76B15, 65M99

Submitted to: *Nonlinearity*

1. Introduction

Thermal bath models such as Langevin dynamics or Nosé-Hoover dynamics are widely used techniques for maintaining the canonical distribution in molecular simulation. Simple thermal baths allow the simulation of bidirectional energy flow, whereas more complicated methods can be designed to provide momentum transfer (barostats) or mimic relaxation processes (generalized Langevin dynamics). As there are natural parallels between turbulent fluids and molecular dynamics, it is interesting to adapt these techniques to hydrodynamics applications. In this paper, as a first step, we consider an artificial thermal bath for semi-discretized partial differential equations, specifically the Burger's and KdV equations.

Molecular dynamics (in the common use of the term) has the structure of a finite dimensional Hamiltonian system, with a total energy function that is a function of positions and momenta. Under typical conditions (the so-called *NVT ensemble*), the volume of the simulation cell is restricted and the number of atoms is fixed, and these may be assumed to share energy equally (equipartition). The system is assumed to be immersed within a larger system (and freely exchanging energy with it) and the energy of the entire system including thermal bath is assumed to remain fixed. In this situation, Gibbs proposed that the microstates of the isolated system will be distributed according to the law

$$\rho_\beta \propto e^{-\beta H},$$

where H is the Hamiltonian (total energy function) of the subsystem, meaning that the invariant measure of the extended system has an associated density which, when integrated out with respect to the bath degrees of freedom, is proportional to ρ_β. The Gibbs (canonical) distribution is only rigorous for special systems in the so-called thermodynamic limit ($N \to \infty$, $V \to \infty$, N/V fixed); for typical systems such as molecular liquids or proteins, the Gibbs distribution is often assumed and is the starting point for simulation. In order to maintain the canonical distribution in simulation, various devices are used. The *sampling* problem refers to the calculation of averages of given functions with respect to a specified invariant (equilibrium) distribution. Molecular models may involve constraints (for example fixing the distance between two atoms) or modifications such as those required to model an imposed environmental pressure, so the form of the Gibbs distribution is often modified in practice to reflect such considerations.

In the case of the Gibbs distribution, or, more generally, any distribution defined by a suitably bounded smooth, positive density function, we have a few choices for the mechanism by which sampling is achieved. The Monte-Carlo method [1] is an iteration strategy that combines a randomly generated step with a Metropolis-Hastings accept/reject condition in order to guarantee that the points generated have the desired distribution. In some cases, for example with steep molecular potentials, Monte-Carlo methods may experience large numbers of rejected steps, which can lead to an inefficient sampling of the phase space. Moreover, the sequence of points generated by a Monte-Carlo method has no temporal correlation. For these reasons, molecular modellers often rely on dynamical approaches or the use of stochastic differential equations. These techniques generate paths in phase space which can be used to calculate thermodynamic averages under an ergodic hypothesis: the assumption that the path emanating from any particular initial condition densely covers the relevant portion of phase space with an appropriate probability density. The ergodicity of stochastic dynamics sampling methods such as Brownian or Langevin dynamics can be demonstrated by showing that the adjoint *generator* (i.e. the *Fokker-Planck*, or *Kolmogorov forward* operator) is elliptic or, more generally, hypoelliptic [2, 3, 4, 5, 6, 7].

An alternative to Langevin dynamics often used in molecular simulations is the Nosé-Hoover thermostat [8, 9, 10] which modifies Newtonian dynamics to include an auxiliary variable that provides partial control of the molecular dynamics ensemble; when applied to a sufficiently strongly mixing dynamical system, such deterministic schemes can be effective in practice,

although in order to have a rigorous ergodic property it is necessary to incorporate an additional stochastic perturbation. Generalized thermostat methods which combine auxiliary dynamics with stochastic perturbation are studied in [11, 12, 13, 14].

1.1. Thermostats and PDE models

The foundation for studying the motions of a fluid dynamics model by reference to an invariant distribution has been considered by a variety of authors [15, 16, 17, 18, 19, 20, 21, 22, 23, 24, 25], and there is numerical evidence that these systems typically evolve near thermodynamic equilibrium [26, 27, 28, 29]. Thus it is also natural to consider adapting the thermostatting methodologies to partial differential equations (or their semi-discrete analogues). Equilibrium statistical mechanics is largely dictated by the conservation laws of the system. These constrain the probability space and enter directly into the invariant measure. For partial differential equations, the discretization in space destroys or modifies some or all of the conservation laws, and thereby the invariant measure, resulting in numerical bias [28, 29]. This creates a potential application for thermostats which is distinct from their motivation in the molecular dynamics setting: they may allow the correction of defects in the distribution due to spatial discretization.

For example, for 2D ideal fluids, the most comprehensive mean field equilibrium theory yields the Miller-Robert-Sommeria (MRS) measure [20, 21, 22, 23], which is grounded in the conservation of the full infinite family of vorticity invariants of the Euler equations. By contrast, standard numerical methods preserve total energy, and at most two of the vorticity invariants. Consequently, when the dynamics of such a system is ergodic, its invariant measure is necessarily significantly different from the MRS measure. (Possible exceptions are the sine-bracket truncation [30] and particle methods [29].)

In addition to perturbing the invariant measure, models for fluids involve dynamics at a range of spatio-temporal scales, and in particular, there may be no clear scale separation. Additionally, there is usually a downscale cascade of vorticity and in some cases kinetic energy, i.e. a secular tendency to excite motion on ever smaller scales: the phenomena known as turbulence. Spatial discretization must arrest this cascade and some sort of closure model (either implicit in the discretization or explicitly modelled and parameterized) is necessary. The choice of closure has consequences for statistical mechanics, and it may be desirable to restore the invariant distribution to correct for the numerical bias. Hence, solely for the purpose of correcting thermodynamic calculations for discretization effects, there is a need to study thermostatting methods in the context of partial differential equations. In Section 2 of this article, we describe a general framework for treating semi-discrete PDEs using a reasonably general thermostatting methodology.

1.2. Weak thermostats and accurate dynamical approximation

In the setting of fluids modelling, there can be an additional issue in play. While it can be said that much of molecular modelling is solely focused on the recovery of Gibbs averages, the purpose of simulation in fluids is more often to model dynamics in the vicinity of a Gibbs state. The thermostats used in PDEs may thus be viewed as model corrections to maintain the environment for a dynamical simulation. The requirements of: (1) fast convergence to the invariant distribution (as needed to efficiently compute ensemble averages) and (2) minimal disturbance of the short term time dynamics (as needed for accurately computing correlations) are mutually competing ones, and the design of a good thermostat implies a choice in the tradeoff between these. For this reason, we discuss the concept of a *weak* thermostat.

In the meteorology literature, DelSole [31] observed that the covariance matrix of a variable

satisfying a smooth deterministic ordinary differential equation must take the form

$$C(\tau) = C_0 + \tau S + \tau^2 A + \cdots$$

with S a skew-symmetric and A a symmetric matrix. By comparison, the covariance matrix of a variable satisfying a multivariate Ornstein-Uhlenbeck process must take the form

$$C(\tau) = C_0 \exp(\tau \tilde{A}),$$

where $\tilde{A}$ is a (different) symmetric matrix with nonpositive eigenvalues.

In particular, a stochastic process $\eta(t)$ is mean-square differentiable if there exists a function $\dot{\eta}(t)$ such that the expectation

$$\lim_{\varepsilon \to 0} \left\langle \left[\frac{\eta(t+\varepsilon) - \eta(t)}{\varepsilon} - \dot{\eta}(t) \right]^2 \right\rangle = 0$$

holds in mean-square sense. This derivative is consistent with the deterministic concept. The solution of a smooth dynamical system is differentiable, whereas that of a stochastic differential equation is not so. For accurate computation of dynamical quantities, mean-square differentiability is a desirable property for thermostated dynamics.

Recently, Leimkuhler, Noorizadeh and Penrose [32] have proposed a criterion for assessing the efficiency of a thermostat as a function of the above two criteria. Their analysis in the context of Hamiltonian dynamics showed that the velocity auto-correlation function (VAF) of Nosé-Hoover-Langevin (NHL) dynamics [12] scales as $c(\tau) = 1 - \kappa_2 \tau^2$ in the limit of small correlation times τ, just as the unperturbed dynamics. By comparison, for Langevin dynamics the VAF scales as $c(\tau) = 1 - \kappa_1 \tau$ in this limit. In particular, this implies that VAFs under Langevin dynamics have the wrong curvature at $\tau = 0$, making accurate computation of auto-correlations impossible. For NHL dynamics the noise process is only present in the differential equation for the auxiliary thermostat variable; hence it is integrated once before influencing the momenta variables (and twice before influencing the positions). Consequently the noise in the NHL dynamics takes the form of a memory term or colored noise process and allows for a more accurate computation of correlations.

We mention in passing that another potential application in which the trade-off between fast sampling and accurate dynamics can be expected to play a prominent role is the application of the fluctuation-dissipation theorem to determine the sensitivity of an invariant measure to perturbations in the underlying dynamics [33, 34, 35]. The non-equilibrium response of a system to a small change in its vector field is computed from correlation functions in the unperturbed equilibrium measure. To do so it is necessary both to ensure that the numerical simulation samples the correct measure, and at the same time to perturb the system as little as possible, while allowing the accurate computation of temporal autocorrelations.

1.3. Results for the Burgers and KdV equations

Herein, we apply stochastic-dynamical thermostats to truncated PDE models, in the form of discretized nonlinear wave equations, under the restrictions: (1) that the finite dimensional phase flow is divergence-free, and that (2) the invariant measure is a smooth function of the conserved quantities of the finite dimensional flow (possibly conditional on δ-function measures involving additional conserved quantities).

We demonstrate weakly coupled thermal regulation techniques in the setting of the inviscid Burgers-Hopf (BH) and Korteweg-de Vries (KdV) models

$$u_t + u u_x + \mu u_{xxx} = 0, \tag{1}$$

where $\mu = 0$ for BH and $\mu > 0$ for KdV. Both equations are one-dimensional models inheriting the quadratic nonlinearity of fluid motion. The models share a bi-Hamiltonian structure and

are formally integrable. However, classical solutions of the Burgers-Hopf equation fail to exist for all time, whereas solutions of the the KdV equation remain smooth. Finite truncation of the BH and KdV models typically breaks integrability. Truncated BH models exhibit chaos and decorrelation of modes on a range of different time scales, and as such it has been used in the literature as a highly simplified model representative of certain aspects of climate [36, 37, 38]. In contrast, truncated solutions of the KdV model may be supposed to retain KAM tori, obstructing ergodicity, and making it a good test model for thermostatting. The truncated BH/KdV models preserve discrete approximations to the first three integrals of the bi-Hamiltonian hierarchy, i.e. the momentum $\mathcal{M} = \int u \, dx$, kinetic energy $\mathcal{E} = \int \frac{1}{2} u^2 \, dx$, and Hamiltonian $\mathcal{H} = \int \frac{1}{6} u^3 - \frac{\mu}{2} u_x^2 \, dx$.

In a series of papers, [36, 37, 38] Majda and co-workers studied the equilibrium statistical mechanics of finite difference and spectral discretizations of the Burgers-Hopf equation ($\mu = 0$), discussing the associated conservation laws and weak invariant sets, and their relation to ergodicity. They computed pdfs of the spectral coefficients, mean spectra, and time-correlation functions. Since the BH equation can be written as a Hamiltonian system in two distinct forms, the definition of the Gibbs measure $\rho \propto \exp(-\beta H)$ depends on the choice of Hamiltonian. Abramov et al. [38] choose the linear Poisson bracket and cubic Hamiltonian, for which the associated Gibbs measure is unbounded. However, since their deterministic dynamics also preserves a quadratic invariant, the resulting product measure (the Gibbs measure restricted to a level set of a hypersphere) does define a probability measure. In this paper we introduce a perturbation to the Burgers/KdV model to ensure ergodic sampling of this measure, $\rho \propto \exp(-\beta H)\delta(E - E_0)\delta(M)$, where $H \approx \mathcal{H}$, $E \approx \mathcal{E}$ and $M \approx \mathcal{M}$, and E_0 is the initial energy.

1.4. Ergodicity

For the truncated incompressible Navier-Stokes equation, E and Mattingly [39] proved ergodicity under highly degenerate stochastic forcing of just two modes in the low wave number range, with viscous damping at the large wave number end of the spectrum. Their proof requires establishing a Lyapunov function and verifying the Hörmander condition for their drift and diffusion vector fields. Our concept of thermostatting is meant to provide a realistic model for the interaction of a semidiscrete PDE with the unresolved high modes of the full (infinite) representation, thus we introduce thermostatting only in the high modes and have in effect a situation opposite to that of E and Mattingly. Nevertheless we show that their method based on commutators could in principle be applied in the present instance, were the phase space is flat. In fact our vector fields (in the case of a N-mode truncation) are confined to the tangent space of the $(2N - 1)$-dimensional hypersphere, so that the calculation of high order brackets becomes extremely involved. We therefore rely on numerical experiments to verify the ergodic property and show that the expected density is obtained with a high degree of accuracy.

The remainder of this paper is laid out as follows. In Section 2 we introduce the thermostat techniques and discuss the relevant theory. In Section 3 we describe the pseudospectral truncations of the BH and KdV equations, present their equilibrium statistical mechanics, discuss ergodicity in the context of thermostatting, and propose some perturbation vector fields. Results with the thermostated dynamics of the BH and KdV are presented in Section 4. Discussion and conclusions are given in Section 5.

2. Thermostats

In this section we discuss thermostats in the context of finite-dimensional Hamiltonian systems. In particular we encounter noncanonical Hamiltonian systems with multiple conserved

quantities. We discuss the statistical mechanics of general Hamiltonian systems by introducing microcanonical, canonical and mixed canonical distribution functions. To sample the mixed canonical distribution function we discuss the use of a generalized thermostat method for the Hamiltonian system with conserved quantities and consider its theoretical foundation (in particular the ergodicity property).

2.1. Finite-dimensional Hamiltonian dynamics and statistical mechanics

Consider a Hamiltonian system on $\mathbf{R}^d$, i.e. an initial value problem of the form

$$\frac{\mathrm{d}X}{\mathrm{d}t} = f(X) \equiv J \nabla H(X), \qquad X(t) \in \mathcal{D} \subset \mathbf{R}^d, \quad X(0) = X_0, \tag{2}$$

where $J = -J^T$ is a constant skew-symmetric matrix, $H(X) : \mathcal{D} \to \mathbf{R}$ is the Hamiltonian, and ∇ denotes the vector of partial derivatives with respect to X. The Poisson bracket is an abstract geometrical object associated with the form J and defined by

$$\{F, G\} := \nabla F(X)^T J \nabla G(X), \tag{3}$$

for arbitrary functions $F(X)$, $G(X) : \mathcal{D} \to \mathbf{R}$. Note that the time derivative of a function $F(X(t)) : \mathcal{D} \to \mathbf{R}$ along a solution to (2) is given by

$$\frac{\mathrm{d}F}{\mathrm{d}t} = \{F, H\}.$$

Evident from the antisymmetry of the Poisson bracket, $H(X)$ is invariant under the flow, since $dH/\mathrm{d}t = \{H, H\} = 0$. In fact, it can be easily checked that any function $\mu(H(X))$ is also invariant. More generally, a first integral of the system is a function $I(X)$ such that

$$\{I, H\} = \nabla I(X)^T J \nabla H(X) = 0.$$

The Hamiltonian vector field $f(X)$ defines a flow on $\mathbf{R}^d$. A probability density function $\rho(X, t) : \mathcal{D} \times \mathbf{R} \to \mathbf{R}$, satisfying $\rho(X, t) \geq 0$, $\int \rho(X, t) \, \mathrm{d}X = 1, \forall t$, is transported under the Hamiltonian flow according to

$$\frac{\partial}{\partial t}\rho(X, t) + \nabla \cdot \rho(X, t)f(X) = 0. \tag{4}$$

Equilibrium statistical mechanics is concerned with stationary solutions of (4). An equilibrium pdf is a solution of

$$\nabla \cdot \rho(X)f(X) = 0.$$

It may be readily checked that the vector field $f(X)$ associated with (2) is divergence-free, $\nabla \cdot f(X) = 0$, in which case the above relation simplifies to

$$f(X) \cdot \nabla \rho(X) = 0. \tag{5}$$

It follows that $\rho(X)$ is itself a first integral of the flow ($\{\rho, H\} = 0$). In particular, if (2) admits precisely $J + 1$ independent first integrals H, I_1, ..., I_J, then any equilibrium pdf must be a function of these:

$$\rho(X) = \rho(H(X), I_1(X), \cdots, I_J(X)). \tag{6}$$

On the other hand, it is clear that any such function ρ that depends on X only through its invariants is stationary under (4).

For a system of particles in thermal contact with a heat reservoir, such that energy is exchanged at constant temperature, volume and mass, the likelihood of states is given by the canonical Gibbs density

$$\rho(X) \propto \exp(-\beta H(X)), \tag{7}$$

where β is the inverse temperature. When more invariants are present, this pdf may be generalized to

$$\rho(X) \propto \exp(-\beta H(X) - \beta_1 I_1(X) - \cdots - \beta_J I_J(X)). \tag{8}$$

For the Gibbs measure to define a pdf, it has been assumed that the function is normalizable, i.e. there exists a finite proportionality constant such that $\int \rho(X)\,\mathrm{d}X = 1$.

More generally, one can define an equilibrium pdf as a generalized function, such as the singular measure

$$\rho(X) \propto \delta(H(X) - H^0)\,\delta(I_1(X) - I_1^0)\cdots\delta(I_J(X) - I_J^0), \tag{9}$$

where δ is the Dirac distribution. In statistical physics this pdf is referred to as the microcanonical ensemble and specifies the relative probabilities of various microstates of a system at fixed values of energy, volume and mass (as well as the other first integrals). It is a stationary solution to (4) only in a weak sense.

In some cases it is useful to define a mixed canonical-microcanonical measure such as

$$\rho(X) \propto \exp\left(-\beta H(X)\right)\delta(I_1(X) - I_1^0)\cdots\delta(I_J(X) - I_J^0). \tag{10}$$

For example, [38] investigated the statistics of finite-truncations of the Burgers-Hopf equation in a pdf of the form

$$\rho(X) \propto \exp(-\beta H(X))\delta(E(X) - E_0)\delta(M(X)), \tag{11}$$

where the level sets of a quadratic invariant E define compact subspaces upon which the Gibbs measure (in the cubic Hamiltonian, see Appendix Appendix A) can be normalized.

The expectation of an observable $F(X)$ under the measure $\rho(X)$ is defined as the ensemble average

$$\langle F \rangle = \int_{\mathcal{D}} F(X)\rho(X)\,\mathrm{d}X = \int_{\mathcal{D}} F(X)\,\nu(\mathrm{d}X)$$

for some proper measure ν such that $\nu \geq 0$ and $\int_{\mathcal{D}} \nu(\mathrm{d}X) = 1$. In general the approximation of such an integral by numerical quadrature is prohibitively expensive due to the large dimension of X encountered in practical applications. Instead Metropolis Monte-Carlo methods are frequently used to compute expectation, despite their slow convergence rate. Such methods give us no information about the dynamics of (2) however.

An equilibrium distribution ρ is practically meaningful when it is the density of the unique invariant measure ν under (4). Let $\Phi_t(X)$ denote the time-t flow map of (2), and denote by $\Phi_t^n(X)$, its nth iterate. We say the flow of (2) *samples* the distribution ρ if the iterates $\{\Phi_t^n(X), n \in \mathbf{Z}\} \sim \rho$, for almost all t and almost all X. In particular, if the flow is ergodic with respect to $\rho(X)$, then for almost every initial condition X_0, the solution to (2) samples the equilibrium density ρ, and the time average

$$\bar{F} = \lim_{T \to \infty} \frac{1}{T} \int_0^T F(X(t))\,\mathrm{d}t$$

equals the ensemble average $\bar{F} = \langle F \rangle$.

We remark that solutions to the transport equation (4) starting from a smooth, nonstationary initial density function $\rho(X,0)$ do not asymptotically approach a steady state in the sense of classical solutions, due to lack of diffusion. However, they may converge weakly to an equilibrium measure (for example, a uniform measure with compact support on a proper subset of the kinetic energy manifold may converge weakly to the uniform measure on the whole manifold).

The autocorrelation function $c(\tau)$ of observable $F(X)$ is defined by

$$c(\tau) = \frac{\langle F(\Phi_\tau X) F(X) \rangle}{\langle F(X)^2 \rangle}.$$

If the flow is ergodic, the autocorrelation can be computed from the time average according to

$$c(\tau) = c_0^{-1} \lim_{T \to \infty} \frac{1}{T} \int_0^T F(X(t)) F(X(t+\tau)) \, \mathrm{d}t, \qquad c_0 = \lim_{T \to \infty} \frac{1}{T} \int_0^T F(X(t))^2 \, \mathrm{d}t.$$

2.2. Generalized Bulgac-Kusnezov thermostats

A typical trajectory of (2) cannot ergodically sample a distribution like (7) due to preservation of the Hamiltonian H. Therefore, in molecular dynamics a number of mechanisms have been introduced to model the thermal exchange with the reservoir, so perturbing the Hamiltonian vector field that typical trajectories of the perturbed dynamics do ergodically sample (7).

One such approach is Langevin dynamics, in which balanced stochastic noise and dissipation are added to the Hamiltonian flow, such that the desired measure becomes the unique, globally attracting invariant measure of the associated Fokker-Planck equations. A generalized form of Langevin dynamics that perturbs (2) such that it samples the Gibbs distribution (7) is

$$\mathrm{d}X = f(X) \, \mathrm{d}t - \frac{\beta \sigma^2}{2} \nabla H(X) \, \mathrm{d}t + \sigma \, \mathrm{d}W,$$

where $W(t)$ is a vector of independent Wiener processes. One limitation of this approach is that it destroys all invariants of the original system. In order to retain some of these it would be necessary to introduce constraint projections which would also create significant difficulties in discretization. It is well known that additive noise is much easier to treat accurately in discretization than multiplicative noise.

Another approach, proposed by Nosé [8, 9] and Hoover [10], involves the introduction of an auxiliary variable, embedding the Hamiltonian flow in a higher dimensional phase space, such that the projected dynamics on the original phase space is (one hopes) ergodic. The deterministic approach is often non-ergodic, however, motivating the inclusion of Langevin forcing of the auxiliary variable [11]. Nosé-Hoover type schemes can be expanded to include multiple auxiliary variables and more general couplings than originally conceived; a broadened framework was proposed in [14] and termed Generalized Bulgac-Kusnetzov (GBK) thermostatting. In the simplest form of a GBK thermostat, we augment the system (2) with a small number of additional variables ξ_k, $k = 1, \ldots, d_T$, and perturbation vector fields which for our purposes may be assumed to be linear in the ξ_k. Let $g_k(X) : \mathcal{D} \to \mathbf{R}^d$, $k = 1, \ldots, d_T$, be smooth vector fields. The complete system is then a set of coupled ordinary and stochastic differential equations of the form:

$$\mathrm{d}X = f(X)\mathrm{d}t + \sum_{k=1}^{d_T} \xi_k g_k(X)\mathrm{d}t, \tag{12}$$

$$\mathrm{d}\xi_k = h_k(X)\mathrm{d}t - \gamma \xi_k \mathrm{d}t + \sigma \mathrm{d}w_k, \quad k = 1, \ldots, d_T, \tag{13}$$

where the $w_k(t)$ are independent scalar Wiener processes. The number of thermostat variables d_T is typically small, say $d_T = 1$ or $d_T = 2$, so the computational cost of simulating the thermostatted system is essentially equivalent to that of simulating the physical model.

Recall that the Ornstein-Uhlenbeck (OU) process

$$\mathrm{d}\xi = -\gamma \xi \mathrm{d}t + \sigma \mathrm{d}w \tag{14}$$

has analytical solution

$$\xi(t) = e^{-\gamma t} \xi(0) + \sigma \sqrt{\frac{1 - e^{-2\gamma t}}{2\gamma}} \Delta w,$$

where $\Delta w \sim \mathcal{N}(0, 1)$. Choosing $\gamma = \alpha \sigma^2 / 2$, the normal distribution with mean zero and variance α^{-1}, i.e.

$$\vartheta(\xi) = \sqrt{\frac{\alpha}{2\pi}} \exp\left(\frac{-\alpha}{2}\xi^2\right),\tag{15}$$

satisfies the stationary Fokker-Planck equation

$$\gamma \frac{\partial}{\partial \xi}\vartheta(\xi)\xi + \frac{1}{2}\sigma^2 \frac{\partial^2}{\partial \xi^2}\vartheta(\xi) = 0.\tag{16}$$

In particular, it is well known that the density (15) is the unique, globally attracting, steady state solution of the Fokker-Planck equation associated to (14). Hence, solutions of (14) ergodically sample (15).

Of course our interest is not in the simple Ornstein-Uhlenbeck equation but in (12)-(13). Given a desired distribution $\rho(X)$, we seek $h_k(X) : \mathbf{R}^d \to \mathbf{R}$, $k = 1, \ldots, d_T$, such that the product distribution

$$\pi(X, \xi) = \rho(X)\vartheta(\xi)\tag{17}$$

is a stationary solution of the Fokker-Planck equation associated with (12)–(13), i.e.

$$\nabla \cdot \pi(X, \xi)\left(f(X) + \sum_k \xi_k g_k(X)\right)$$
$$+ \sum_k \left[\frac{\partial}{\partial \xi_k}(\pi(X, \xi)(h_k(X) - \gamma \xi_k)) - \frac{\sigma^2}{2}\frac{\partial^2}{\partial \xi_k^2}\pi(X, \xi)\right] = 0.\tag{18}$$

We proceed formally, assuming a smooth density of the general form (6), but note that for singular measures such as (10), the above requirement must be satisfied in an appropriate weak sense. The case when the measure depends on a subset of I_j via a Dirac distribution will be handled later.

For concreteness, let $\rho(X) = \exp(-F(X))$, where $F(X) = F(H(X), I_1(X), \ldots, I_J(X))$ is differentiable with respect to all of its arguments, and denote $\beta_0(X) = \partial F/\partial H$ and $\beta_j(X) = \partial F/\partial I_j$, $j = 1, \ldots, J$. The expression (18) simplifies under the conditions $\nabla \cdot f = 0$ and $\nabla H \cdot f = \nabla I_j \cdot f = 0$. Additionally using the fact that the terms of the OU process (14) satisfy the stationary Fokker-Planck equation (16), the relation (18) reduces to

$$0 = \sum_k \xi_k \nabla \cdot \pi(X, \xi)g_k(X) + h_k(X)\frac{\partial}{\partial \xi_k}\pi(X, \xi),$$

$$= \sum_k \xi_k \pi(X, \xi)\nabla \cdot g_k(X) - \xi_k \pi(X, \xi)\left(\beta_0 \nabla H + \sum_{j=1}^J \beta_j \nabla I_j\right) \cdot g_k(X)$$
$$- \alpha \xi_k \pi(X, \xi)h_k(X),$$

$$= \sum_k \xi_k \left(\nabla \cdot g_k(X) - \left(\beta_0 \nabla H + \sum_{j=1}^J \beta_j \nabla I_j\right) \cdot g_k(X) - \alpha h_k(X)\right).$$

Hence it is sufficient to take

$$h_k(X) = \frac{1}{\alpha}\left(\nabla \cdot g_k(X) - \left(\beta_0 \nabla H + \sum_{j=1}^J \beta_j \nabla I_j\right) \cdot g_k(X)\right)$$

for a given vector field $g_k(X)$. For the Gibbs distribution (7), $h_k(X)$ reduces to

$$h_k(X) = \frac{1}{\alpha}\left(\nabla \cdot g_k(X) - \beta \nabla H \cdot g_k(X)\right).\tag{19}$$

We have yet to specify the vector fields g_k. The construction of this section ensures that the target distribution is invariant under the thermostated Fokker-Planck operator for any choice of g_k.

2.3. The ergodic property

The previous derivation of the GBK method ensures that the augmented probability distribution π is invariant under the Fokker-Planck flow associated with the GBK dynamics (12)–(13). To ensure correct sampling, one must also show that π is the density of the unique ergodic invariant measure. By construction, (12)–(13) define a phase flow under which the density π is invariant. The associated measure is positive for all open sets on the phase space. Hence, to show uniqueness and thereby ergodicity, it suffices to show that the Fokker-Planck operator associated to (12)–(13) is hypoelliptic, which follows from the controllability condition due to Hörmander [3, 5, 4, 7, 6].

Hörmander's condition can be tailored slightly for the GBK thermostat, as demonstrated next. Let $\mathcal{L}(V_0, V_1, \ldots, V_{d_T})$ denote the ideal of the vector fields V_k with $k > 0$ within the Lie algebra generated by all of the V_k:

$$\mathcal{L}(V_0, V_1, \ldots, V_{d_T}) = \{V_{k_0}, [V_{k_0}, V_{k_1}], [[V_{k_0}, V_{k_1}], V_{k_2}], \ldots\},$$

where $[\cdot, \cdot]$ denotes the commutator of vector fields, k_0 takes values in the set $\{1, \ldots, d_T\}$, and k_1, k_2, etc. take values in $\{0, \cdots, d_T\}$. Denoting by ∂_{ξ_k} the unit vector in $\mathbf{R}^{d+d_T}$ corresponding to the variable ξ_k, Hörmander's condition [2] to ensure a smooth probability measure for this system is

$$\mathbf{R}^{d+d_T} \subset \operatorname{span} \mathcal{L}(F, \partial_{\xi_1}, \ldots, \partial_{\xi_{d_T}}),$$

where

$$F = \begin{pmatrix} f(X) + \sum_k \xi_k g_k(X) \\ h_1(X) - \gamma \xi_1 \\ \vdots \\ h_{d_T}(X) - \gamma \xi_{d_T} \end{pmatrix}$$

denotes the deterministic vector field of (12)–(13). Defining

$$G_k = [F, \partial_{\xi_k}] = \begin{pmatrix} g_k(y) \\ -\gamma \partial_{\xi_k} \end{pmatrix}, \quad k = 1, \ldots, d_T, \tag{20}$$

we find that

$$[F, G_k] = \begin{pmatrix} [f, g_k] \\ 0 \end{pmatrix} + c_1 G_k + c_2(X) \partial_{\xi_k}. \tag{21}$$

Since the unit vectors ∂_{ξ_k} form a globally defined basis for the auxiliary space of the thermostat variables ξ_k, it remains to construct a basis for the original space $\mathbf{R}^d$. Eliminating the ξ_k and the G_k from (21), shows that the following reduced Hörmander condition holds:

Lemma 1 *The GBK method (12)–(13) satisfies Hörmander's condition at a point* $(X, \xi_1, \ldots, \xi_{d_T}) \in \mathbf{R}^{d+d_T}$ *if the related Hörmander condition on* $\mathbf{R}^d$ *holds at* X*:*

$$\mathbf{R}^d \subset \operatorname{span} \mathcal{L}(f, g_k; k = 1, \ldots, d_T).$$

When choosing appropriate vector fields g_k, it is important to ensure that f and the g_k do not all share an invariant manifold of co-dimension one. For example, in the case $d_T = 1$, $g = g_1$, if $\mathcal{N} = \{X \in \mathcal{D} \,|\, \eta(X) = 0\}$ defines a smooth invariant manifold such that $\nabla \eta(X) \cdot f(X) = \nabla \eta(X) \cdot g(X) = 0$ for all $X \in \mathcal{N}$, then it follows that

$$f, g \in T_X \mathcal{N} \quad \Rightarrow \quad [f, g] \in T_X \mathcal{N},$$

and consequently, the Lie algebra will be rank deficient on $\mathcal{N}$, and Hörmander's condition will fail there. Furthermore, if $\mathcal{N}$ is of co-dimension one, it may partition the phase space.

When constructing thermostats for a mixed measure such as (10) we take advantage of the just noted symmetry of the Lie algebra. That is, we choose the perturbation vector fields $g_k(X)$ to satisfy $\nabla I_j \cdot g_k(X) = 0$, $\forall j, k$, and subsequently determine the $h_k(X)$ to ensure the invariance of the smooth part of the measure (10), according to (19).

To choose the $g_k(X)$, one can either appeal to underlying symmetries of the Hamiltonian vector field (2), or make use of a projector onto the tangent bundle of the manifold defined by intersection of the conditions $I_j(X) = I_j^0$, $j = 1, \ldots, J$. Let $A(X) \in \mathbf{R}^{d \times d_T}$ denote the matrix whose columns are the gradients of the first integrals $I_j(X)$:

$$A(X) = (\nabla I_1, \cdots, \nabla I_J),$$

and assume A has full column rank. Then for a given perturbation vector field $\tilde{g}(X)$, the projected vector field

$$g(X) = (I - A(A^T A)^{-1} A^T)\tilde{g}(X) \tag{22}$$

preserves the invariants I_j.

3. Semidiscrete PDE models

To illustrate the application of thermostats to PDEs, we select two related model problems, the inviscid Burgers-Hopf (BH) and Korteweg-De Vries (KdV) equations. We choose these models as simple one-dimensional problems with features in common with more sophisticated fluid models, i.e. quadratic nonlinearity, multiple conserved quantities, a tendency to generate fine scale dynamics from smooth initial conditions, and slow (fast) decorrelation times for low (high) wave numbers.

The BH/KdV model (1) is discretized using a pseudospectral truncation (see Appendix Appendix A), resulting in an equation of the form (cf. A.14)

$$\frac{\partial}{\partial t} u_N + \frac{1}{2} \frac{\partial}{\partial x} \mathcal{P}_N(u_N^2) + \mu \frac{\partial^3}{\partial x^3} u_N = 0, \tag{23}$$

where $u_N := \mathcal{P}_N u(x)$ is the projection of the function u onto N Fourier modes.

The truncated model retains as first integrals the discrete analogs of $\mathcal{M}$, $\mathcal{E}$ and $\mathcal{H}$, respectively [36]:

$$M = \int_0^{2\pi} u_N \, dx, \tag{24}$$

$$E = \frac{1}{2} \int_0^{2\pi} u_N^2 \, dx, \tag{25}$$

$$H = \int_0^{2\pi} \frac{1}{6} u_N^3 - \frac{\mu}{2} \left(\frac{\partial}{\partial x} u_N \right)^2 \, dx. \tag{26}$$

3.1. Statistical mechanics of the truncated model

Abramov et al. [38] proposed a statistical mechanics for the pseudospectral truncation of the Burgers-Hopf equation, which carries over to the KdV equation. The spectral representation of (23) is (cf. A.15)

$$\frac{d\hat{u}_n}{dt} = \hat{f}_n(\hat{u}) = -\frac{in}{2} \left(\sum_{|n-m| \leq N} \hat{u}_{n-m} \hat{u}_m \right) + in^3 \mu \hat{u}_n, \qquad |n|, |m| \leq N, \tag{27}$$
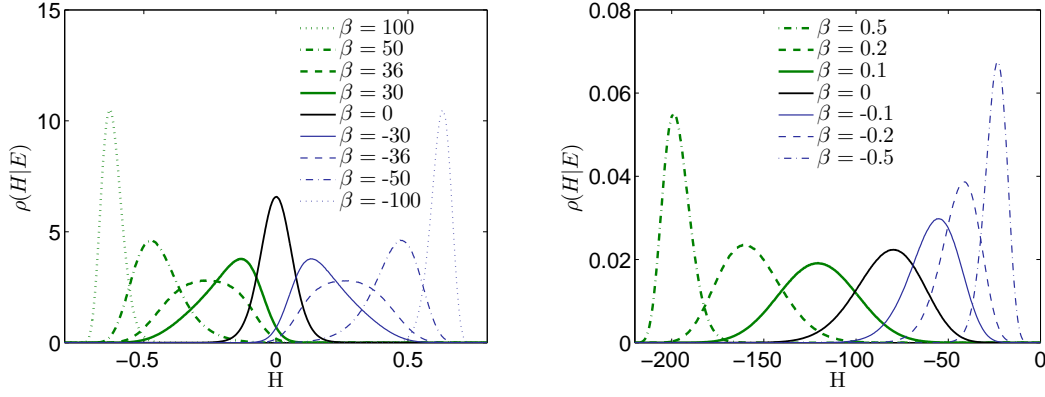
Figure 1: Probability density functions of the Hamiltonian $H(\hat{u})$ for different values of β, $E_0 = 1$. Left: BH equation. Right: KdV equation.

where $\hat{u}, \hat{f} \in \mathbf{C}^{2N+1}$, $\hat{u}_{-n} = \hat{u}_n^*$. First note that the vector field $\hat{f}(\hat{u})$ is divergence-free:

$$\nabla \cdot \hat{f}(\hat{u}) = 2\mathrm{Re} \sum_{|n| \leq N} \frac{\partial}{\partial \hat{u}_n} \hat{f}_n = 2\mathrm{Re} \sum_{|n| \leq N} -in\hat{u}_0 + in^3\mu = 0,$$

since $\hat{u}_0 \in \mathbf{R}$ for a real smooth 2π-periodic function $u(x)$. This implies that an equilibrium density is a function of the conserved quantities

In [38] it is noted that a Gibbs-like density $\rho(\hat{u}) = \exp(-\beta H(\hat{u})) - \gamma E(\hat{u}))$ cannot be normalized due to the unboundedness of level sets of the highest order terms in H. Noting that level sets of E are hyperspheres when $M = 0$, and hence compact, [38] instead propose a mixed ensemble that is microcanonical in E and M, and canonical in H, i.e.

$$\rho(\hat{u}) \propto \exp(-\beta H(\hat{u}))\delta(E(\hat{u}) - E_0)\delta(M(\hat{u})).$$

We adopt this density here. Since the phase space is compact, the system supports both positive and negative regimes for the statistical temperature β^{-1} [15].

We used the Metropolis-Hastings algorithm to compute probability density functions of the Hamiltonian H for $E_0 = 1$ and different values of β. The pdfs shown in Figure 1 were obtained using 10^8 samples and $N = 15$. Because the phase space is compact the temperature assumes both positive and negative values. For the Burgers-Hopf equation we note that the skewness varies in a nonlinear way as a function of β, but that the pdfs are anti-symmetric with respect to $\beta = 0$. For the KdV equation the pdf with $\beta = 0$ has negative skewness and it changes to positive near the value $\beta = 0.1$.

In Figure 2 we plot expectation values of the kinetic energy spectrum $|\hat{u}_n|^2$ as a function of wave number n. Note that the energy is equipartitioned for $\beta = 0$ which corresponds to the case of a uniform distribution on the sphere $\delta(E(\hat{u}) - E_0)$. For the Burgers-Hopf equation we observe significant tilt in the spectrum for values $\beta \neq 0$. More energy resides in the large scales (small wave numbers). Furthermore, the spectra are identical for opposite signed β. For the KdV equation we observe opposite tilt in the spectrum depending on the sign of β, with more energy at low wave numbers for $\beta < 0$ and at high wave numbers for $\beta > 0$.
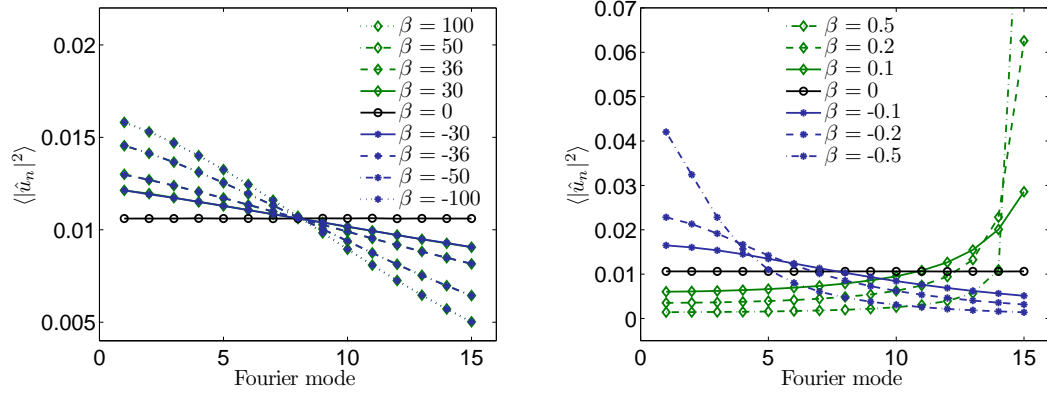
Figure 2: Mean kinetic energy spectrum, for different values of β. Left: BH equation. Right: KdV equation.

3.2. Ergodicity of stochastic hydrodynamics models

For the truncated incompressible Navier-Stokes equation, E and Mattingly [39] proved ergodicity under highly degenerate stochastic forcing of just two modes in the low wave number range, with viscous damping at the large wave number end of the spectrum. The proof of [39] requires establishing a Lyapunov function and verifying the Hörmander condition for the drift and diffusion vector fields.

In this paper we use GBK thermostats [14] to effect a simple non-dissipative closure model, with forcing implemented at the small scales/large wave numbers. Because the thermostats control the flux of energy into and out of the system, they do not require a separate dissipation term to maintain stability. Here we illustrate through analysis that thermostatting the small scales (essentially through "backscatter") can be effective, i.e. we show the Hörmander condition for this type of forcing. Our starting point is the GBK method (12)–(13) on $\mathbf{C}^{2N+1} \times \mathbf{R}^{d_T}$.

The form of Lemma 1 suggests adapting the analysis of E and Mattingly to Burgers' equation, and forcing at large wave numbers. We next derive a suitable set of perturbation vector fields $\hat{g}_1, \ldots, \hat{g}_M$ that ensure Hörmander's condition.

The truncated Burgers/KdV model (27) is derived in Appendix Appendix A. For the rest of this section we restrict our attention to the case $\mu = 0$ of Burgers' equation, because the formulas are simpler, and the dispersion term does not contribute to mixing between distinct wave numbers. Following [39], define $\hat{u}_n = a_n + ib_n$, and denote the unit vectors in the respective real coordinates by ∂_{a_n} and ∂_{b_n}. Then

$$\hat{f}_n = -\frac{in}{2} \sum_{|m-n|<N} (a_{n-m} + ib_{n-m})(a_m + ib_m)$$

$$= \frac{n}{2} \sum_{|m-n|<N} (a_{n-m}b_m + a_m b_{n-m})\partial_{a_n} + (b_{n-m}b_m - a_{n-m}a_m)\partial_{b_n}.$$

Since the solution $u(x,t)$ of the Burgers/KdV model is real valued, the Fourier modes $\hat{u}_n$ satisfy $\hat{u}_{-n} = \hat{u}_n^*$, which in turn implies the conditions $a_{-n} = a_n$ and $b_{-n} = -b_n$. We also assume $\hat{u}_0 \equiv \hat{f}_0 \equiv 0$.

Fixing $n > 0$ for the moment, define the index sets $N_n^+ = \{n+1, \ldots, N\}$ and $N_n^- =$

$\{1, \ldots, n-1\}$, and note that

$$
\begin{aligned}
m \in N_n^+ &\quad\Rightarrow\quad m > 0, n - m < 0, \\
m \in N_n^- &\quad\Rightarrow\quad m > 0, n - m > 0, \\
m \in (n - N_n^+) &\quad\Rightarrow\quad m < 0, n - m > 0.
\end{aligned}
$$

With this in mind, the vector field $\hat{f}_n$ is written as

$$
\hat{f}_n = \frac{n}{2} \sum_{m \in N_n^-} (a_{n-m} b_m + a_m b_{n-m}) \partial_{a_n} + (b_{n-m} b_m - a_{n-m} a_m) \partial_{b_n} +
$$

$$
\frac{n}{2} \sum_{m \in N_n^+} (a_{m-n} b_m - a_m b_{m-n}) \partial_{a_n} + (-b_{m-n} b_m - a_{m-n} a_m) \partial_{b_n} +
$$

$$
\frac{n}{2} \sum_{m \in (N_n^+ - n)} (-a_{n+m} b_m + a_m b_{n+m}) \partial_{a_n} + (-b_{n+m} b_m - a_{n+m} a_m) \partial_{b_n},
$$

where now all indices are positive. Furthermore, it can be checked that the last two sums are equivalent, so the formula simplifies to

$$
\hat{f}_n = \frac{n}{2} \sum_{m \in N_n^-} (a_{n-m} b_m + a_m b_{n-m}) \partial_{a_n} + (b_{n-m} b_m - a_{n-m} a_m) \partial_{b_n} +
$$

$$
n \sum_{m \in N_n^+} (a_{m-n} b_m - a_m b_{m-n}) \partial_{a_n} + (-b_{m-n} b_m - a_{m-n} a_m) \partial_{b_n}.
$$

Next we compute commutators with the canonical unit vectors, for future reference. (These are the columns of the Jacobian matrix of $\hat{f}$.) We find:

$$
X_\ell = [\hat{f}, \partial_{a_\ell}] = n(b_{n-\ell} - b_{\ell-n} + b_{\ell+n}) \partial_{a_n} + n(-a_{n-\ell} - a_{\ell-n} - a_{\ell+n}) \partial_{b_n},
$$

$$
Y_\ell = [\hat{f}, \partial_{b_\ell}] = n(a_{n-\ell} + a_{\ell-n} - a_{\ell+n}) \partial_{a_n} + n(b_{n-\ell} - b_{\ell-n} - b_{\ell+n}) \partial_{b_n},
$$

where henceforth it is understood that the index of each term is either an element of the set $\{1, \ldots, N\}$, or the term itself is neglected, meaning that each expression in parentheses above has at least one and at most two (when $\ell + m \leq N$) nontrivial terms.

The commutators of X_ℓ and Y_ℓ with respect to generic unit vectors ∂_{a_m} and ∂_{b_m} are:

$$
\begin{aligned}
[X_\ell, \partial_{a_m}] &= n(-\delta_{n-\ell,m} - \delta_{\ell-n,m} - \delta_{\ell+n,m}) \partial_{b_n} \\
&= -(m+\ell) \partial_{b_{m+\ell}} - (\ell-m) \partial_{b_{\ell-m}} - (m-\ell) \partial_{b_{m-\ell}}, \\
[X_\ell, \partial_{b_m}] &= (m+\ell) \partial_{a_{m+\ell}} - (\ell-m) \partial_{a_{\ell-m}} + (m-\ell) \partial_{a_{m-\ell}}, \\
[Y_\ell, \partial_{a_m}] &= (m+\ell) \partial_{a_{m+\ell}} + (\ell-m) \partial_{a_{\ell-m}} - (m-\ell) \partial_{a_{m-\ell}}, \\
[Y_\ell, \partial_{b_m}] &= (m+\ell) \partial_{b_{m+\ell}} - (\ell-m) \partial_{b_{\ell-m}} - (m-\ell) \partial_{b_{m-\ell}},
\end{aligned}
$$

where $\delta_{m,\ell}$ is the Kronecker delta.

If the unit vector ∂_{a_ℓ} is an element of the Lie algebra $\mathcal{L}(\hat{f}, \hat{g}_1, \ldots, \hat{g}_K)$ (hereafter simply denoted by $\mathcal{L}$), then so is X_ℓ. Likewise, inclusion of ∂_{b_ℓ} implies that of Y_ℓ. As a result, we have the following inclusions:

$$
\begin{aligned}
\partial_{a_\ell}, \partial_{a_m} \in \mathcal{L} &\Rightarrow (\partial_{b_{|\ell-m|}} \pm \partial_{b_{\ell+m}}) \in \mathcal{L}, \\
\partial_{a_\ell}, \partial_{b_m} \in \mathcal{L} &\Rightarrow (\partial_{a_{|\ell-m|}} \pm \partial_{a_{\ell+m}}) \in \mathcal{L}, \\
\partial_{b_\ell}, \partial_{b_m} \in \mathcal{L} &\Rightarrow (\partial_{b_{|\ell-m|}} \pm \partial_{b_{\ell+m}}) \in \mathcal{L},
\end{aligned}
$$

where the second term on the right in each relation is present only if $\ell + m \leq N$. From the last of these three recursions, it immediately follows that if ∂_{b_1} is in $\mathcal{L}$, so are all of the ∂_{b_ℓ}. If additionally $\partial_{a_1} \in \mathcal{L}$, then from the second implication above, all of the ∂_{a_ℓ} also follow, and the

Hörmander condition is satisfied. Hence, to demonstrate the Hörmander condition, it suffices to thermostat only the lowest wave number, taking $\hat{g}_1 = \partial_{a_1}$, $\hat{g}_2 = \partial_{b_1}$.

On the other hand, directly thermostatting the low wave numbers is likely to be intrusive in the dynamics. Instead we wish to thermostat the highest wave numbers, which constitute an uncertain component in the solution anyway. If ∂_{a_N} and $\partial_{a_{N-1}}$ are in $\mathcal{L}$, then we obtain $\partial_{b_1} \in \mathcal{L}$ from the commutator $[X_N, \partial_{a_{N-1}}]$, and subsequently all of the ∂_{b_ℓ} and associated Y_ℓ. Finally, the commutator $[Y_N, \partial_{a_{N-1}}]$ yields $\partial_{a_1} \in \mathcal{L}$, subsequently all of the ∂_{a_ℓ}, and Hörmander is again satisfied. Therefore, we can construct a GBK thermostat satisfying Hörmander's condition for Burgers' equation and perturbations only to the real parts of the two highest wave numbers, taking $\hat{g}_1 = \partial_{a_N}$, $\hat{g}_2 = \partial_{a_{N-1}}$. Combining this with a Lyapunov function would ensure ergodicity in the measure $\rho(X) = \exp(-\beta E(X))$, where E is the quadratic invariant of Burgers/KdV.

The above approach will not allow sampling of a mixed measure (11), however, since the perturbation vector fields so defined do not lie in the tangent bundle to the hypersphere of constant kinetic energy E. Instead, we may choose a single perturbation vector field $\hat{g}$ that is a rotation about one or more coordinate axes, for example,

$$\hat{g} = b_N \partial_{a_N} - a_N \partial_{b_N}. \tag{28}$$

Since both $\hat{f}$ and $\hat{g}$ are defined in the tangent space to the manifold of constant E, the Lie algebra generated by these vectors also preserves the first integral. The phase space is compact, and ergodicity follows from the Hörmander condition. However, with quadratic $\hat{f}$ and linear $\hat{g}$, the commutators are all quadratic or higher in order, making this condition difficult to check. Instead we include numerical experiments to assess ergodicity.

3.3. Thermostated dynamics for the semidiscrete model

In this section we specify the thermostated dynamics in the context of the truncated BH/KdV equation (23) and the mixed canonical distribution (11). The GBK thermostat for equation (23) and a single thermostat variable ξ is:

$$\mathrm{d}u_N = f_N(u_N)\mathrm{d}t + \xi g_N(u_N)\mathrm{d}t, \tag{29}$$

$$\mathrm{d}\xi \;\; = 2\operatorname{Re} h(u_N)\mathrm{d}t - \gamma\xi\mathrm{d}t + \sigma\mathrm{d}w, \tag{30}$$

where $f_N(u_N) = -\frac{1}{2}\frac{\partial}{\partial x}\mathcal{P}_N(u_N^2) - \mu\frac{\partial^3}{\partial x^3}u_N$. The function $g(u_N)$ is chosen such that its projection $g_N(u_N) := \mathcal{P}_N g(u_N)$ satisfies the constraints

$$\int_0^{2\pi} \frac{\delta M}{\delta u_N} g_N(u_N)\,\mathrm{d}x = 0, \quad \int_0^{2\pi} \frac{\delta E}{\delta u_N} g_N(u_N)\,\mathrm{d}x = 0. \tag{31}$$

These relations constrain the dynamics to the Dirac distributions on M and E. Taking into account that $\mathcal{P}_N$ is symmetric, the constraints (31) reduce to

$$\int_0^{2\pi} g(u_N)\,\mathrm{d}x = 0, \quad \int_0^{2\pi} u_N g(u_N)\,\mathrm{d}x = 0. \tag{32}$$

Without loss of generality one may assume $M = 0$, since the nonzero case may be handled with a change of variables. Furthermore, in spectral representation this condition takes the simple form $\hat{u}_0 \equiv 0$, which can be easily enforced by simply neglecting the constant mode in the spectral representation, taking $\hat{u} = (\hat{u}_n; 1 \le |n| \le N)$.

To preserve the kinetic energy constraint we either choose $g(u_N)$ to respect the rotation symmetry, as in (28), or use a projection such as (22).

For a given function $\tilde{g}(u_N)$, using the definitions (24) and (25) of M and E, and taking $M = 0$, we observe that the function

$$g(u_N) = \tilde{g}(u_N) - \frac{1}{2\pi}\int_0^{2\pi}\tilde{g}(u_N)\,\mathrm{d}x - \frac{1}{2E}u_N\int_0^{2\pi} u_N\tilde{g}(u_N)\,\mathrm{d}x \tag{33}$$

satisfies the constraints (32). In spectral representation, $\hat{g}_0 = 0$ and

$$\hat{g}_n(\hat{u}) = \frac{1}{2\pi} \int_0^{2\pi} g(u_N) e^{-inx} \, dx, \qquad 1 \le |n| \le N.$$

Using (19) we compute $h(\hat{u})$ from

$$h(\hat{u}) = \frac{1}{\alpha} \left(\nabla_{\hat{u}} \cdot \hat{g}(\hat{u}) - \beta \nabla_{\hat{u}} H(\hat{u}) \cdot \hat{g}(\hat{u}) \right).$$

The gradient of the Hamiltonian $H(\hat{u})$ is

$$\frac{\partial H(\hat{u})}{\partial \hat{u}_n} = \int_0^{2\pi} \frac{\delta H}{\delta u_N} \frac{\partial u_N}{\partial \hat{u}_n} \, dx = \int_0^{2\pi} \frac{\delta H}{\delta u_N} e^{inx} \, dx = 2\pi \left(\widehat{\frac{\delta H}{\delta u_N}} \right)^*_n, \quad 1 \le |n| \le N,$$

which yields

$$\nabla_{\hat{u}} H(\hat{u}) \cdot \hat{g}(\hat{u}) = \sum_{1 \le |n| \le N} \frac{\partial H(\hat{u})}{\partial \hat{u}_n} \hat{g}_n(\hat{u})$$

$$= 2\pi \sum_{1 \le |n| \le N} \left(\widehat{\frac{\delta H}{\delta u_N}} \right)^*_n \hat{g}_n(\hat{u}) = \int_0^{2\pi} \frac{\delta H}{\delta u_N} g_N(u_N) \, dx.$$

The spectral representation of $h(u_N)$ follows:

$$h(\hat{u}) = \frac{1}{\alpha} \left(\nabla_{\hat{u}} \cdot \hat{g}(\hat{u}) - 2\pi\beta \sum_{1 \le |n| \le N} \left(\widehat{\frac{\delta H}{\delta u_N}} \right)^*_n \hat{g}_n(\hat{u}) \right).$$

For each value of $1 \le |n| \le N$:

$$\frac{\partial \hat{g}_n(\hat{u})}{\partial \hat{u}_n} = \frac{1}{2\pi} \int_0^{2\pi} \frac{\partial g(u_N)}{\partial u_N} \frac{\partial u_N}{\partial \hat{u}_n} e^{-inx} \, dx = \frac{1}{2\pi} \int_0^{2\pi} \frac{\partial g(u_N)}{\partial u_N} \, dx.$$

This gives us

$$h(u_N) = \frac{1}{\alpha} \left(\frac{N}{\pi} \int_0^{2\pi} \frac{\partial \tilde{g}(u_N)}{\partial u_N} \, dx - \frac{N}{E} \int_0^{2\pi} u_N \tilde{g}(u_N) \, dx - \beta \int_0^{2\pi} \frac{\delta H}{\delta u_N} g_N(u_N) \, dx \right).$$

4. Numerical study

We rely on a series of numerical simulations to test the performance of the thermostats mentioned above in the setting of the Burgers and KdV equations. Our interest here is in two crucial issues: (i) the ergodic nature of the extended SDE models, even under limited contact with the stochastic heat bath, and (ii) the degree to which thermodynamic corrections alter dynamic observables (e.g. temporal correlation functions). In evaluating the experimental results, we use the terminology from Subsection 2.1 and explicitly define the autocorrelation functions of the real part of the Fourier modes, i.e.

$$c_n(\tau) = C \lim_{\tau \to \infty} \tau^{-1} \int_0^{\tau} \text{Re}\{\hat{u}_n(t+\tau)\} \text{Re}\{\hat{u}_n(t)\} dt, \qquad n = 1, \ldots, N, \qquad (34)$$

where C is a suitable normalization constant so that $c_n(0) = 1$.

4.1. Burgers' equation

In our computations we set $N = 15$, $E_0 = 1$ and $\beta = -30$. We solve equations (29)–(30) in time by applying a Strang splitting method, thus dividing the calculation into two steps: (1) the solution of the equation for the auxiliary variable, and (2) the solution of the equations governing Fourier coefficients of the solution. The stochastic differential equation for the auxiliary variable can be solved exactly when u_N is fixed, whereas in step (2) the system for u_N is treated using the implicit midpoint rule (a scheme which preserves quadratic first integrals, i.e. the hypersphere).

The numerical method is

$$\xi^* = e^{-\gamma \frac{\tau}{2}} \xi^0 + \frac{2\mathrm{Re}h(u_N^0)}{\gamma}\left(1 - e^{-\gamma \frac{\tau}{2}}\right) + \sigma\sqrt{\frac{1 - e^{-\gamma\tau}}{2\gamma}}\Delta w^0,$$

$$u_N^1 = u_N^0 + \tau f_N(u_N^{1/2}) + \tau\xi^* g_N(u_N^{1/2}), \qquad u_N^{1/2} := \frac{u_N^1 + u_N^0}{2},$$

$$\xi^1 = e^{-\gamma \frac{\tau}{2}} \xi^* + \frac{2\mathrm{Re}h(u_N^1)}{\gamma}\left(1 - e^{-\gamma \frac{\tau}{2}}\right) + \sigma\sqrt{\frac{1 - e^{-\gamma\tau}}{2\gamma}}\Delta w^1,$$

where $\Delta w^0, \Delta w^1 \sim \mathcal{N}(0, 1)$ and τ is a time step.

The first question concerns the ergodic sampling of the target distribution. This can depend on the choice of g. We let $\tilde{g}(u_N) = u_N^2$. With this particular choice of function $\tilde{g}(u_N)$ from expression (33) we find

$$g(u_N) = u_N^2 - \frac{1}{2\pi}\int_0^{2\pi} u_N^2\,\mathrm{d}x - \frac{1}{2E}u_N\int_0^{2\pi} u_N^3\,\mathrm{d}x$$

and compute

$$h(u_N) = -\frac{1}{\alpha}\left(\frac{N}{E}\int_0^{2\pi} u_N^3\,\mathrm{d}x + \beta\int_0^{2\pi}\frac{\delta H}{\delta u_N}g_N(u_N)\,\mathrm{d}x\right).$$

Numerical results are presented in Figure 3. In the computations we used 10^9 data points and $\tau = 0.001$. In Figure 3 we compare the numerically computed histogram of $H(\hat{u})$ and the spectrum to the Monte Carlo simulations using the Metropolis-Hastings algorithm. Since a single trajectory produces what is essentially a perfect Hamiltonian pdf and spectrum we infer that the method is ergodic.

We then set about constructing a thermostat that controls the invariant measure using only forcing at high wave numbers. To this end we work with a spectral representation of $g(u_N)$. For any skew-Hermitian matrix $B(\hat{u})$ the vector field

$$\hat{g}(\hat{u}) = B(\hat{u})\hat{u}$$

is norm preserving and therefore retains the first integral E. We choose matrix B such that it only acts on the large wave number Fourier coefficients, i.e.

$$\hat{g}(\hat{u})_n = \begin{cases} 0, & |n| < n^*, \\ i\,\mathrm{sign}(n)\hat{u}_n, & |n| \geq n^*, \end{cases} \tag{35}$$

and refer to this method as GBK(n^*). In this case the effect of the perturbation is to directly modify the phase of only the $(N - n^* + 1)$ highest Fourier modes. This can be contrasted directly with the approach of E & Mattingly [39], who stochastically force the lowest modes of a truncated Navier-Stokes model using a Langevin approach. Here we thermostat at the finest scales, effectively controlling the measure through backscatter.

The results for $n^* = 11$ are shown in Figure 4 using 10^9 data points. All computations are done with $\tau = 0.01$. These results again suggest that the method is ergodic. Not only can we
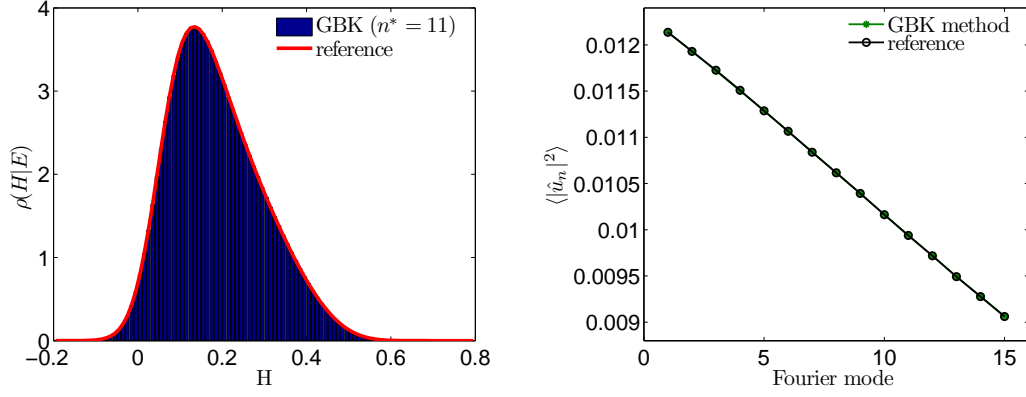
Figure 3: Gentle thermostatting of BH equation with GBK method, taking $\tilde{g}(u_N) = u_N^2$, $\alpha = 30$ and $\gamma = 20$. Left: probability density function of $H(\hat{u})$. Right: mean kinetic energy spectrum.
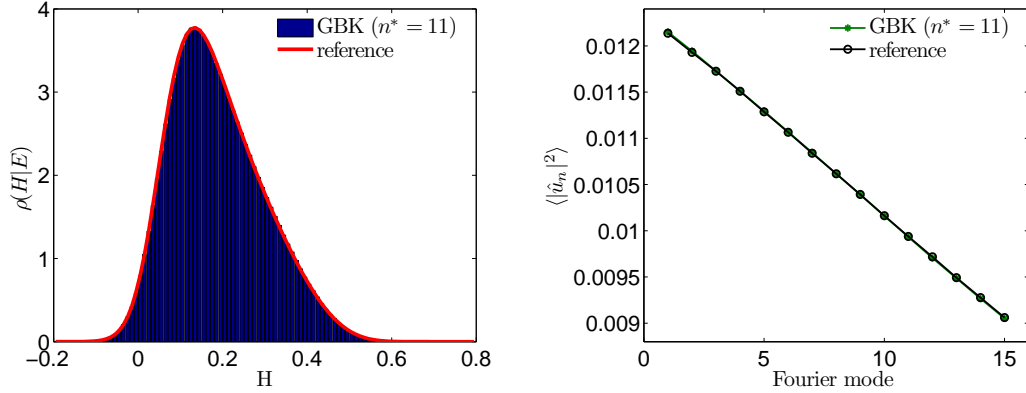

Figure 4: Gentle thermostatting of BH equation with GBK($n^* = 11$) method, $\alpha = \gamma = 1$. Left: probability density function of $H(\hat{u})$. Right: mean kinetic energy spectrum.

get away with thermostatting directly only the highest five wave numbers, it is in fact possible to control the distribution using only a *single mode*. In Figure 5, the pdfs are shown for the real parts of the Fourier coefficients 1, 5, 10 and 15 when only the highest wave number $\hat{u}_{15}$ is directly coupled to the stochastic auxiliary variable ξ. Note that while $E_0 = 1$, the dynamics is constrained to the hypersphere with radius $1/\sqrt{2\pi} \approx 0.4$, and this number bounds the support of the pdfs.

Thermostatting only the high wave numbers leads to a reduced rate of convergence of averages compared to a thermostat that acts directly on all components. This effect can be seen in Figure 6. Slope values are approximate. When plotted as a function of n^* and compared to the least square fitted exponential function in Figure 7 on a logarithmic scale we observe good agreement. This suggests that the rate of convergence decreases exponentially with respect to n^*.

On the other hand, although the convergence rate of averages may be reduced by using a
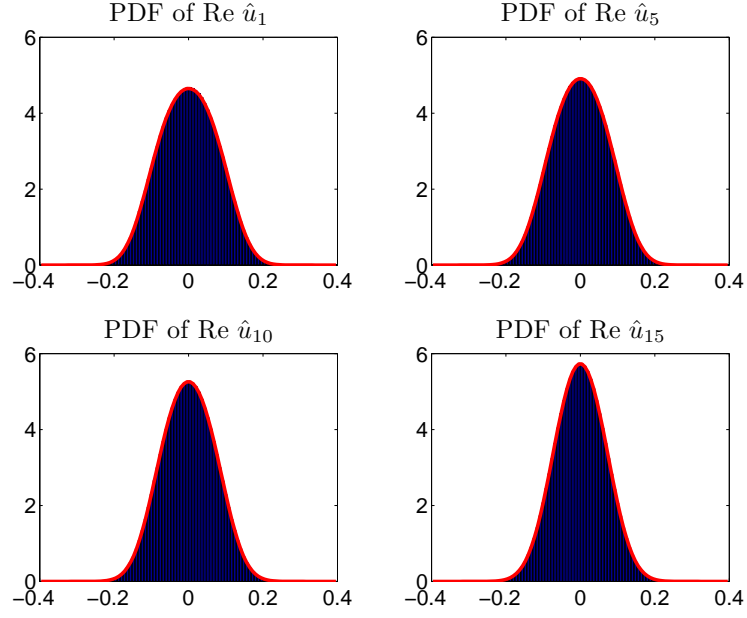
Figure 5: Probability density function of real parts of Fourier coeffiecients 1, 5, 10 and 15. GBK($n^* = 15$) thermostat method compared to reference.
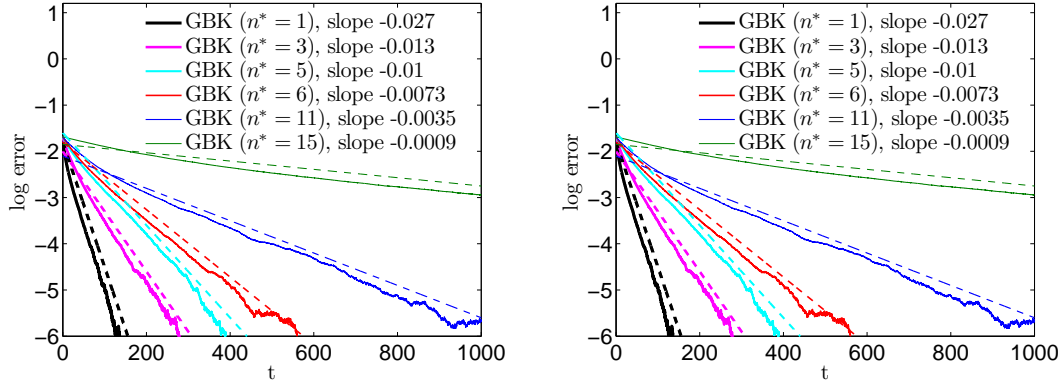

Figure 6: Convergence of the expected value of Hamiltonian for an ensemble of $20\,000$ initial conditions, $\alpha = \gamma = 1$.
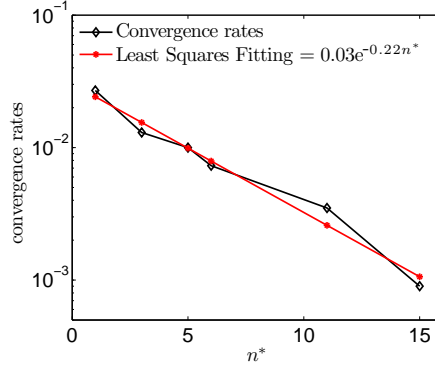
Figure 7: Convergence rates from Figure 6 as a function of n^* and least squares fitting to the exponential function.

weak thermostat, the perturbation of slow dynamics is simultaneously reduced, meaning that where the dynamics of slow variables is relevant, these methods are likely to be of greatest value. As we noted in the introduction, the advantage of the GBK thermostat over direct Langevin thermostating is that the stochastic forcing only influences the original dynamics after integration—as a memory or red noise term—leading to a second order perturbation of autocorrelation functions *of the fast modes* $\hat{u}_n$, $n \geq n^*$. In fact, a straightforward calculations shows that we would expect only third order or higher perturbations to autocorrelations of the slow modes $\hat{u}_n$, $n < n^*$, which are not directly thermostated.

In Figure 8a we plot the L^2 error of the pdf of the Hamiltonian as a function of sampling time, showing the convergence to the reference pdf. We observe the expected sampling convergence rate, $1/2$. In Figures 8b, 8c and 8d we plot L^2 errors, computed on the interval $\tau \in [0, 50]$, as a function of sampling time of the autocorrelation functions $c_1(\tau)$, $c_3(\tau)$ and $c_5(\tau)$, respectively. Observe that the graphs level off indicating a convergence to a limiting value of the net perturbation. (To see that the graph for the method $\text{GBK}(n^* = 15)$ eventually stabilizes, we would have to integrate even longer in time.) Complementary to Figure 8 we plot in Figure 9 the same autocorrelation functions and visually compare them to reference curves. The reference curves are computed using constant Hamiltonian simulations from a mixed canonically distributed ensemble of 10^6 initial conditions.

Note the big differences in errors between $\text{GBK}(n^* = 1)$ and the others in Figure 8b. Only in the case of $\text{GBK}(n^* = 1)$ is the equation for $\text{Re}\,\hat{u}_1$ directly perturbed. This leads to the second order perturbation of autocorrelation function while the other methods, $\text{GBK}(n^* > 1)$, lead to third order or higher perturbations of autocorrelation functions. This can be seen in Figure 9b where we compare the autocorrelation functions $c_1(\tau)$ for two methods, $\text{GBK}(n^* = 1)$ and $\text{GBK}(n^* = 11)$, with the reference curve for the small correlation times τ. It is clearly evident that the method $\text{GBK}(n^* = 11)$ is more accurate than $\text{GBK}(n^* = 1)$.

Interestingly errors in autocorrelation functions also depend on the value of n^*. For larger value of n^* we observe smaller errors, see Figures 8b, 8c and 8d. In Figure 9a it is easy to see that two methods $\text{GBK}(n^* = 3)$ and $\text{GBK}(n^* = 11)$, which do not directly perturb the equation for $\text{Re}\,\hat{u}_1$, have better autocorrelation functions compared to method $\text{GBK}(n^* = 1)$. But it is also notable that the more gentle method, i.e. the $\text{GBK}(n^*)$ method with larger value of n^*, has the more accurate autocorrelation function.

Similar effects of perturbation order to autocorrelation functions can be seen in Figures 8c
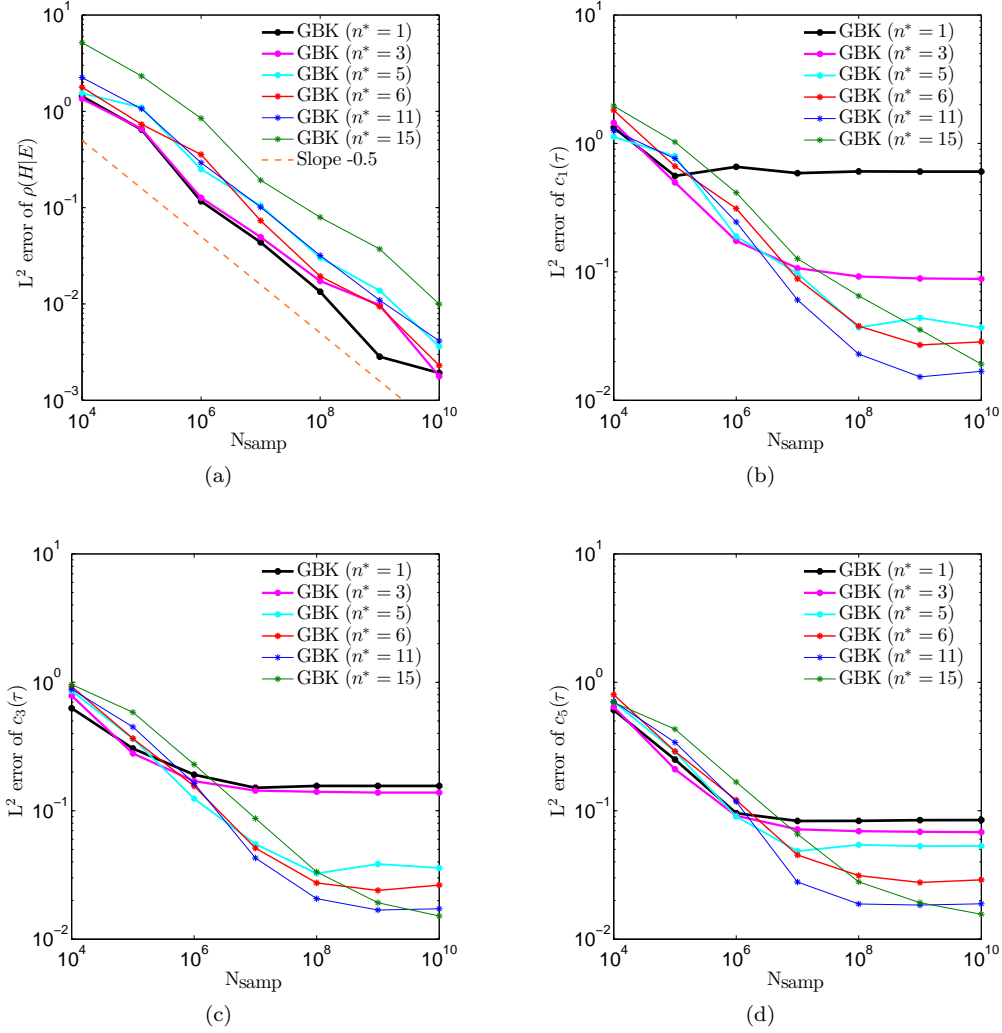
Figure 8: L^2 errors as a function of sampling time with small scale forcing (35) of wave numbers $n \geq n^*$. Top left: evolving pdf of the Hamiltonian, Top right and bottom: autocorrelation functions for $\mathrm{Re}\,\hat{u}_1$, $\mathrm{Re}\,\hat{u}_3$ and $\mathrm{Re}\,\hat{u}_5$. in the evolving pdf of the Hamiltonian, $\alpha = \gamma = 1$.

and 8b. In both methods, GBK($n^* = 1$) and GBK($n^* = 3$), the thermostat variable ξ is directly coupled to the equation for $\mathrm{Re}\,\hat{u}_3$. This gives larger errors compared to the other methods, GBK($n^* > 3$), as seen in Figure 8c. We observe similar trends in the results in Figure 8d. And these translate also to Figures 9c and 9d.

Numerical results presented in Figures 8 and 9 show that the direct coupling to the thermostat ξ in the equations for the slow modes can significantly effect the errors in autocorrelation functions of these modes and vice versa. Since errors in autocorrelation functions decrease with larger value of n^* while, at the same time the convergence rate decreases with larger value of n^* (Figure 6), it suggests seeking n^* to obtain the optimal trade-off between rate of convergence and rate of perturbation to dynamics. (Of course the choice would also depend
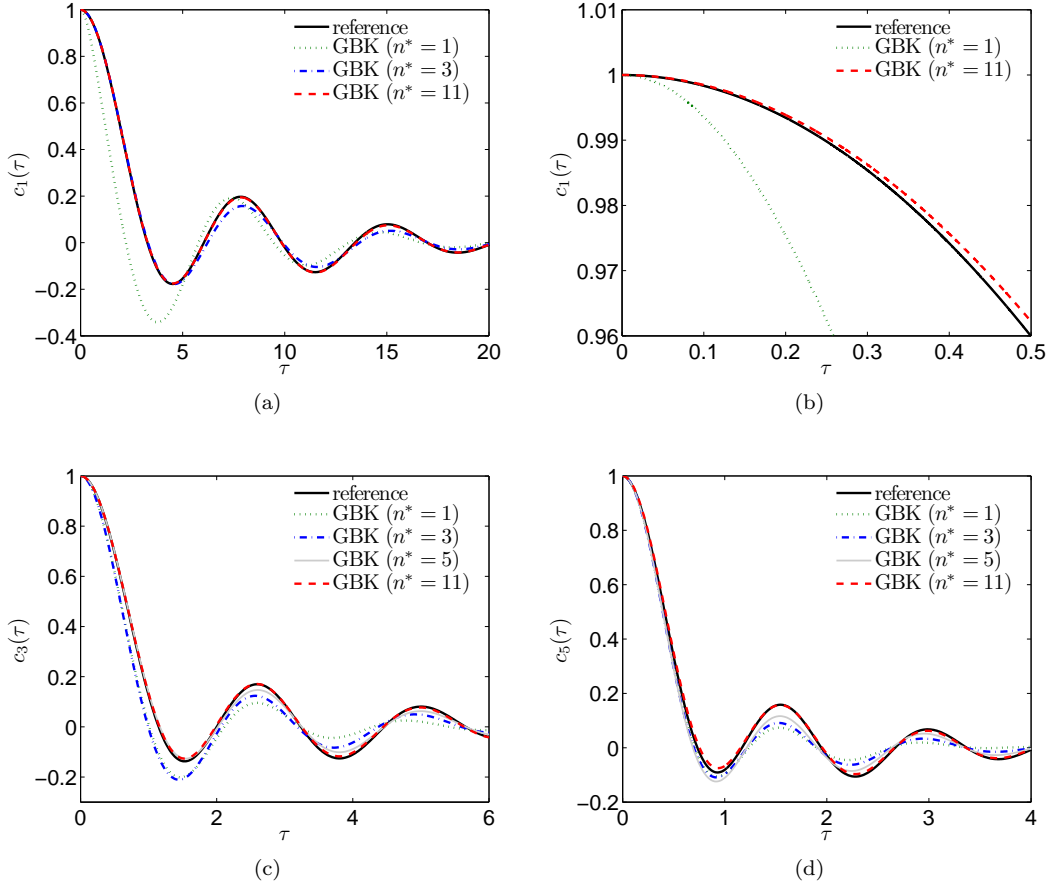
Figure 9: Gentle thermostatting of BH equation with GBK(n^*) method, $\alpha = \gamma = 1$. (a) autocorrelation function $c_1(\tau)$. (b) autocorrelation function $c_1(\tau)$ for small correlation times τ. (c) autocorrelation function $c_3(\tau)$. (d) autocorrelation function $c_5(\tau)$. The reference curves were computed using constant Hamiltonian simulations from a mixed canonically distributed ensemble of 10^6 initial conditions.

on the goal of simulation.)

4.2. Thermostated KdV equation

In the case of the KdV equation we note that the Hamiltonian function $H(\hat{u})$ can be written as the sum of two parts $H = H_1 + H_2$, where

$$H_1(u_N) = \int_0^{2\pi} u_N^3 \, dx, \qquad H_2(u_N) = -\frac{1}{2} \int_0^{2\pi} \left(\frac{\partial}{\partial x} u_N \right)^2 \, dx.$$

The Hamiltonian systems generated by $H_1(u_N)$ and $H_2(u_N)$ each conserves the first integrals M and E individually. Now we consider the following GBK thermostated KdV equation:

$$\frac{\partial}{\partial t} u_N = -\frac{\partial}{\partial x} \mathcal{P}_N \frac{\delta H}{\delta u_N} - \xi \frac{\partial}{\partial x} \mathcal{P}_N \frac{\delta H_2}{\delta u_N} = -\frac{\partial}{\partial x} \mathcal{P}_N \frac{\delta H_1}{\delta u_N} - (1+\xi) \frac{\partial}{\partial x} \mathcal{P}_N \frac{\delta H_2}{\delta u_N},$$
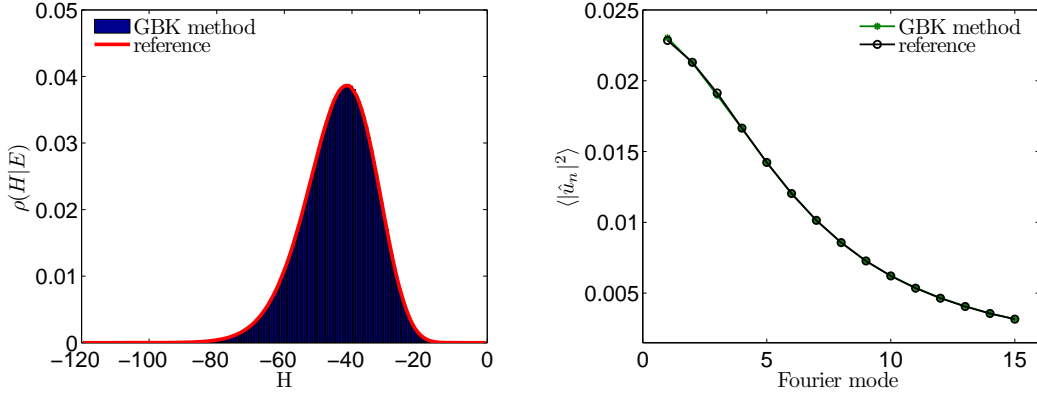
Figure 10: Gentle thermostatting of KdV equation with GBK method, $\alpha = 15$ and $\gamma = 40$. Left: probability density function of $H(\hat{u})$. Right: mean kinetic energy spectrum.

$$d\xi = 2\frac{\beta}{\alpha}\text{Re}\int_0^{2\pi} \frac{\delta H_1}{\delta u_N}\frac{\partial}{\partial x}\mathcal{P}_N\frac{\delta H_2}{\delta u_N}\,dx dt - \gamma\xi dt + \sigma dw,$$

where dw is scalar Wiener process. This approach was suggested in a slightly different form (and for finite dimensional systems only) in [14] and is referred to as a force-perturbation thermostat since it perturbs the 'natural forces' of the system, or rather the balance between these, to realize a thermal control. For the KdV equation we effectively thermostat the system by controlling the strength and direction of dispersion.

To integrate the dynamics numerically in time, we use the following splitting method, which generates a map $(u_N^0, \xi^0) \mapsto (u_N^1, \xi^1)$ with time step τ:

$$\xi^{1/2} = e^{-\gamma\frac{\tau}{2}}\xi^0 + \frac{2}{\gamma}\text{Re}\,h(u_N^0)\left(1 - e^{-\gamma\frac{\tau}{2}}\right) + \sigma\sqrt{\frac{1 - e^{-\gamma\tau}}{2\gamma}}\Delta w^0,$$

$$u_N^* = e^{-(1+\xi^{1/2})\frac{\tau}{2}\frac{\partial^3}{\partial x^3}}u_N^0,$$

$$u_N^{**} = u_N^* + \tau f_N(u_N^{1/2}), \qquad u_N^{1/2} := \frac{1}{2}(u_N^* + u_N^{**}),$$

$$u_N^1 = e^{-(1+\xi^{1/2})\frac{\tau}{2}\frac{\partial^3}{\partial x^3}}u_N^{**},$$

$$\xi^1 = e^{-\gamma\frac{\tau}{2}}\xi^{1/2} + \frac{2}{\gamma}\text{Re}\,h(u_N^1)\left(1 - e^{-\gamma\frac{\tau}{2}}\right) + \sigma\sqrt{\frac{1 - e^{-\gamma\tau}}{2\gamma}}\Delta w^1,$$

where $\Delta w^0, \Delta w^1 \sim \mathcal{N}(0, 1)$. Numerical results with $\tau = 0.001$ are presented in Figures 10–11 (showing, in Figure 10, the convergence of the Hamiltonian probability density function and the spectrum, and, in Figure 11, the autocorrelation functions). 10^9 data points were used to compute the graphs in Figure 10 and 11.

Results from Figure 10 demonstrate that a single trajectory produces what is essentially a perfect Hamiltonian pdf and spectrum, hence we infer that the method is ergodic. On the other hand Figure 11 shows that, for the particular values of α and γ, the GBK method has only a small impact on dynamics as measured by autocorrelation functions.
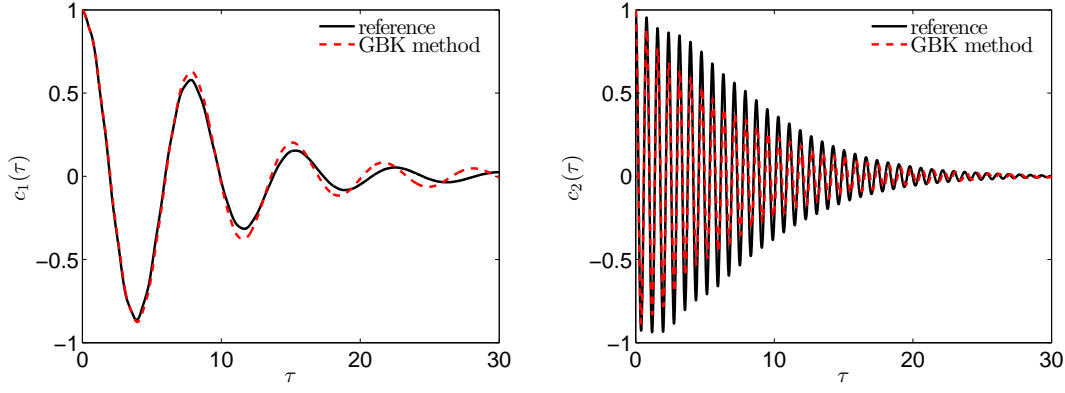
Figure 11: Gentle thermostatting of KdV equation with GBK method, $\alpha = 15$ and $\gamma = 40$. Left: autocorrelation function $c_1(\tau)$. Right: autocorrelation function $c_2(\tau)$. The reference curves were computed using constant Hamiltonian simulations from a mixed canonically distributed ensemble of 10^6 initial conditions.

5. Conclusions

In this paper we have outlined a framework for controlling the invariant measures of discretized PDEs, via coupling to one or more thermostat variables. Ergodicity is guaranteed if the perturbation vector fields satisfy Hörmander's condition.

The convergence rate of the time averages to the ensemble average in the desired measure depends on the strength of the thermostat, which can be controlled either through method parameters, or through choosing the degree of coupling between dynamical and thermostat wave numbers. The strength of the thermostat must be weighed against the degree of perturbation of dynamical quantities such as correlations.

For the example of the Burgers-Hopf equation, we have demonstrated that effective sampling can be achieved with perturbation only to the Fourier mode with largest wave number, providing a simple model of energetic exchange with unresolved modes. In this way the invariant measure is controlled by perturbing the least accurate component of the solution, and without introducing explicit viscous terms, which might suppress an inverse cascade. A test for this framework will come in extending the results to the 2D Euler equations, which is the subject of current work of the authors.

Acknowledgments

Appendix A. Burgers/Korteweg-de Vries model and spectral truncation

The BH and KdV equations can be written in unified form

$$u_t + uu_x + \mu u_{xxx} = 0, \tag{A.1}$$

where the dispersion constant μ is zero for the BH equation and nonzero for the KdV equation. The classical KdV equation is obtained for $\mu = 1/6$ by rescaling time by the same factor. The BH and KdV equation are Hamiltonian PDEs with similar structure, as we briefly review in the next section.

Appendix A.1. Hamiltonian structure and conserved quantities of BH and KdV equations

We consider Hamiltonian PDEs on a function space $\mathcal{U}$ of smooth, 2π-periodic functions equipped with an inner product. The Poisson bracket (3) generalizes to an integral

$$\{\mathcal{F}, \mathcal{G}\} := \int_0^{2\pi} \frac{\delta \mathcal{F}}{\delta u} \mathcal{J} \frac{\delta \mathcal{G}}{\delta u} \, \mathrm{d}x, \qquad \mathcal{F}, \mathcal{G} : \mathcal{U} \to \mathbf{R},$$

i.e. a skew-symmetric, bilinear form acting on functionals on $\mathcal{U}$ and satisfying the Jacobi identity [40]. Here, $u(x,t) \in \mathcal{U}$ is a (possibly vector-valued) function, $\frac{\delta}{\delta u}$ denotes the variational derivative with respect to u, and $\mathcal{J}$ is a (matrix) differential operator, skew-symmetric with respect to the inner product on $\mathcal{U}$. The Hamiltonian PDE is given by

$$\partial_t u = \{u, \mathcal{H}\}. \tag{A.2}$$

Hence the evolution of any functional $\mathcal{F}$ under the dynamics of a Hamiltonian PDE (A.2) obeys the equation

$$\frac{\partial}{\partial t} \mathcal{F} = \{\mathcal{F}, \mathcal{H}\}.$$

A functional $\mathcal{I}$ satisfying $\{\mathcal{I}, \mathcal{H}\} = 0$ is a first integral and constant along classical solutions to (A.2), as long as these exist.

Equation (A.1) has a bi-Hamiltonian structure [40] and is therefore integrable. The Hamiltonian structure we will use here is defined by

$$\mathcal{J} = -\frac{\partial}{\partial x}, \qquad \mathcal{H} = \int_0^{2\pi} \frac{1}{6}u^3 - \frac{\mu}{2}\left(\frac{\partial}{\partial x}u\right)^2 \, \mathrm{d}x. \tag{A.3}$$

Hence the corresponding Poisson bracket is

$$\{\mathcal{F}, \mathcal{G}\} := -\int_0^{2\pi} \frac{\delta \mathcal{F}}{\delta u} \frac{\partial}{\partial x} \frac{\delta \mathcal{G}}{\delta u} \, \mathrm{d}x. \tag{A.4}$$

One conserved quantity of (A.2) is the linear momentum

$$\mathcal{M} = \int_0^{2\pi} u \, \mathrm{d}x, \tag{A.5}$$

which we can assume to be zero up to Galilean change of coordinates.

Equation (A.1) has infinitely many conserved quantities, as mentioned above, depending on the value of μ. For the BH equation ($\mu = 0$), the integral of any function of u is conserved, and in particular the moments

$$\mathcal{I} = \int_0^{2\pi} u^p \, \mathrm{d}x, \quad p = 1, 2, \ldots \tag{A.6}$$

The first of these is the momentum mentioned earlier and assumed to be zero. The second moment represents the kinetic energy

$$\mathcal{E} = \frac{1}{2} \int_0^{2\pi} u^2 \, \mathrm{d}x. \tag{A.7}$$

The third moment is the Hamiltonian $\int u^3$, i.e. (A.3) with $\mu = 0$.

For the KdV equation, the first integrals of the infinite class are given by

$$\mathcal{I}_n = \int_0^{2\pi} P_{2n-1}\left(u, \frac{\partial}{\partial x}u, \frac{\partial^2}{\partial x^2}u, \ldots\right) dx, \quad n = 1, 2, \ldots,$$

where the polynomials P_n are defined recursively [41] by

$$P_1 = u,$$

$$P_n = -\frac{\partial}{\partial x}P_{n-1} + \sum_{m=1}^{n-2} P_m P_{n-m-1}, \qquad n \geq 2.$$

The even-indexed polynomials P_{2n} are exact differentials and thus trivially preserved. The polynomial $P_1(u)$ corresponds to momentum (A.5), $P_3(u)/2$ to the kinetic energy (A.7) and $P_5(u)/2$ to the Hamiltonian functional (A.3) with $\mu = 1/6$. Hence, all three functionals (A.5), (A.7) and (A.3) are conserved quantities of the equation (A.1) for any value of μ.

Appendix A.2. Spectral truncation of BH and KdV equations

As noted by McLachlan [42], the Hamiltonian structure of a PDE can often be retained in a finite dimensional truncation, by taking care to discretize the Poisson bracket and Hamiltonian separately. The Poisson bracket should be truncated such that remains skew-symmetric and, when nonlinear, satisfies the Jacobi identity. The Hamiltonian can be approximated by any consistent finite dimensional truncation. Majda & Timofeyev [36] present such a truncation for the BH equation, and show that it retains as first integrals approximations of (A.6) for $p = 1, 2, 3$. We recall their discretization here and note that it readily extends to the KdV equation.

Let $\mathcal{P}_N$ denote the standard N-mode Fourier projection operator, i.e.

$$f_N := \mathcal{P}_N f(x) = \sum_{|n| \leq N} \hat{f}_n e^{inx}, \tag{A.8}$$

where

$$\hat{f}_n = \frac{1}{2\pi} \int_0^{2\pi} f(x) e^{-inx} dx$$

is the nth Fourier coefficient of the function $f(x)$. Since $f(x)$ is real we have

$$\hat{f}_{-n} = \hat{f}_n^*. \tag{A.9}$$

It can be directly verified that $\mathcal{P}_N$ is symmetric with respect to the L^2 inner product $(\cdot, \cdot)$ and commutes with the derivative operator $\frac{\partial}{\partial x}$. Consequently the composite operator $\frac{\partial}{\partial x}\mathcal{P}_N$ is skew-symmetric with respect to $(\cdot, \cdot)$ and a truncated Poisson bracket (A.4) may be defined by

$$\{\mathcal{F}_N, \mathcal{G}_N\} := -\int_0^{2\pi} \frac{\delta\mathcal{F}_N}{\delta u_N} \frac{\partial}{\partial x} \mathcal{P}_N \frac{\delta\mathcal{G}_N}{\delta u_N} dx. \tag{A.10}$$

The Hamiltonian restricted to the truncated function u_N is given by

$$H = \int_0^{2\pi} \frac{1}{6}u_N^3 - \frac{\mu}{2}\left(\frac{\partial}{\partial x}u_N\right)^2 dx. \tag{A.11}$$

Therefore the finite truncation follows from (A.2):

$$\frac{\partial}{\partial t}u_N = -\frac{\partial}{\partial x}\mathcal{P}_N \frac{\delta H}{\delta u_N}, \tag{A.12}$$

where

$$\frac{\delta H}{\delta u_N} = \frac{1}{2}u_N^2 + \mu\frac{\partial^2}{\partial x^2}u_N. \tag{A.13}$$

That is,

$$\frac{\partial}{\partial t}u_N + \frac{1}{2}\frac{\partial}{\partial x}\mathcal{P}_N(u_N^2) + \mu\frac{\partial^3}{\partial x^3}u_N = 0. \tag{A.14}$$

In terms of Fourier coefficients this can be written

$$\frac{\mathrm{d}\hat{u}_n}{\mathrm{d}t} = -\frac{in}{2}\left(\sum_{|n-m|\leq N}\hat{u}_{n-m}\hat{u}_m\right) + in^3\mu\hat{u}_n = -\frac{in}{2\pi}\frac{\partial H}{\partial \hat{u}_n^*}, \qquad |n| \leq N, \tag{A.15}$$

and the Hamiltonian is

$$H = \frac{\pi}{3}\sum_{\substack{\ell+m+n=0 \\ |\ell|,|m|,|n|\leq N}}\hat{u}_\ell\hat{u}_m\hat{u}_n - \mu\pi\sum_{|\ell|\leq N}\ell^2\hat{u}_\ell\hat{u}_\ell^*.$$

The Poisson bracket (A.10) possesses a Casimir invariant

$$M = \int_0^{2\pi} u_N\,\mathrm{d}x = \hat{u}_0, \tag{A.16}$$

the total momentum, which without loss of generality we assume to be zero.

Additionally the quadratic invariant

$$E = \frac{1}{2}\int_0^{2\pi} u_N^2\,\mathrm{d}x \tag{A.17}$$

is conserved since

$$\begin{aligned}
\{E,H\} &= -\frac{1}{2}\int_0^{2\pi} u_N\frac{\partial}{\partial x}\mathcal{P}_N(u_N^2)\,\mathrm{d}x - \mu\int_0^{2\pi} u_N\frac{\partial^3}{\partial x^3}u_N\,\mathrm{d}x \\
&= \frac{1}{2}\int_0^{2\pi} u_N\frac{\partial}{\partial x}u_N^2\,\mathrm{d}x + \mu\int_0^{2\pi}\left(\frac{\partial}{\partial x}u_N\right)\left(\frac{\partial^2}{\partial x^2}u_N\right)\mathrm{d}x \\
&= \frac{1}{6}\int_0^{2\pi}\frac{\partial}{\partial x}u_N^3\,\mathrm{d}x + \frac{\mu}{2}\int_0^{2\pi}\frac{\partial}{\partial x}\left(\frac{\partial}{\partial x}u_N\right)^2\mathrm{d}x = 0,
\end{aligned}$$

due to symmetry of $\mathcal{P}_N$ and its commutativity with $\frac{\partial}{\partial x}$. In terms of Fourier coefficients,

$$E = 2\pi\sum_{|n|\leq N}\frac{1}{2}\hat{u}_n\hat{u}_n^* = \pi\hat{u}_0^2 + 2\pi\sum_{n=1}^N|\hat{u}_n|^2 = 2\pi\sum_{n=1}^N|\hat{u}_n|^2.$$

To solve (A.14) numerically, we evaluate the nonlinear terms in real space using a standard pseudospectral approach (see, e.g. [43]). Due to cubic terms in the Hamiltonian and the thermostat equation, anti-aliasing requires applying the FFTs on a grid of dimension $4(N+1)$, where N is the number of Fourier modes retained in the truncation. All computations are done for fixed value of $N = 15$.

References

[1] R. E. Caflisch. Monte Carlo and quasi-Monte Carlo methods. *Acta Numerica*, pages 1–49, 1998.

[2] L. C. G. Rogers and D. Williams. *Diffusions, Markov Processes, and Martingales, Vol.2: Itô Calculus*. John Wiley & Sons, 1987.

[3] W. Kliemann. Recurrence and invariant measures for degenerate diffusions. *Annals of Probability*, 15(2):690–707, 1987.

[4] J. C. Mattingly, A. M. Stuart, and D. J. Higham. Ergodicity for SDEs and approximations: locally Lipschitz vector fields and degenerate noise. *Stochastic Processes and their Applications*, 101(2):185–232, 2002.

[5] L. Rey-Bellet. Ergodic properties of Markov processes. In *Open Quantum Systems II*, volume 1881 of *Lecture Notes in Mathematics*, pages 1–39. Springer Berlin / Heidelberg, 2006.

[6] M. Hairer. Convergence of Markov processes. Lecture notes, University of Warwick, 2010.

[7] M. Hairer and J. C. Mattingly. Yet another look at Harris' ergodic theorem for Markov chains. In *Seminar on Stochastic Analysis, Random Fields and Applications VI*, volume 63 of *Progress in Probability*, pages 109–117, 2011.

[8] S. Nosé. A molecular dynamics method for simulations in the canonical ensemble. *Molecular Physics*, 52:255–268, 1984.

[9] S. Nosé. A unified formulation of the constant temperature molecular dynamics methods. *Journal of Chemical Physics*, 81:511, 1984.

[10] W. G. Hoover. Canonical dynamics: Equilibrium phase-space distributions. *Physical Review A*, 31:1695–1697, 1985.

[11] A. A. Samoletov, C. P. Dettmann, and M. A. J. Chaplain. Thermostats for "slow" configurational modes. *Journal of Statistical Physics*, 128(6):1321–1336, 2007.

[12] B. Leimkuhler, E. Noorizadeh, and F. Theil. A gentle stochastic thermostat for molecular dynamics. *Journal of Statistical Physics*, 135(2):261–277, 2009.

[13] G. Bussi, D. Donadio, and M. Parrinello. Canonical sampling through velocity rescaling. *Journal of Chemical Physics*, 126:014101, 2007.

[14] B. Leimkuhler. Generalized Bulgac-Kusnezov methods for the sampling of the Gibbs-Boltzmann measure. *Physical Review*, to appear.

[15] L. Onsager. Statistical hydrodynamics. *Nuovo Cimento (9)*, 6(Supplemento 2, Convegno Internazionale di Meccanica Statistica):279–287, 1949.

[16] D. Lynden-Bell. Statistical mechanics of violent relaxation in stellar systems. *Monthly Notices of the Royal Astronomical Society*, 136:101–121, 1967.

[17] R. H. Kraichnan. Statistical dynamics of two-dimensional flow. *Journal of Fluid Mechanics*, 67:155–175, 1975.

[18] R. Salmon, G. Holloway, and M. C. Hendershott. The equilibrium statistical mechanics of simple quasi-geostrophic models. *J. Fluid Mech.*, 75:691–703, 1976.

[19] G. F. Carnevale and J. S. Frederiksen. Nonlinear stability and statistical mechanics of flow over topography. *J. Fluid Mech.*, 175:157–181, 1987.

[20] J. Miller. Statistical mechanics of Euler equations in two dimensions. *Physical Review Letters*, 65(17):2137–2140, 1991.

[21] J. Miller, P. B. Weichman, and M. C. Cross. Statistical mechanics, Euler's equation, and Jupiter's Red Spot. *Physical Review A*, 45(4):2328–2359, 1992.

[22] R. Robert. A maximum-entropy principle for two-dimensional perfect fluid dynamics. *Journal of Statistical Physics*, 65(3-4):531–553, 1991.

[23] R. Robert and J. Sommeria. Statistical equilibrium states for two-dimensional flows. *Journal of Fluid Mechanics*, 229:291–310, 1991.

[24] R. S. Ellis, K. Haven, and B. Turkington. Nonequivalent statistical equilibrium ensembles and refined stability theorems for most probable flows. *Nonlinearity*, 15(2):239–255, 2002.

[25] F. Bouchet and A. Venaille. Statistical mechanics of geophysical flows. emphasis on analytically solvable problems and geophysical applications. In *Peyresq lecture notes on nonlinear physics, volume 3*. World Scientific, in press.

[26] R. Abramov and A. J. Majda. Statistically relevant conserved quantities for truncated quasi-geostrophic flow. *Proceedings of the National Academy of Science*, 100(7):3841–3846, 2003.

[27] A. J. Majda and X. Wang. *Non-linear dynamics and statistical theories for basic geophysical flows*. Cambridge University Press, Cambridge, 2006.

[28] S. Dubinkina and J. Frank. Statistical mechanics of Arakawa's discretizations. *Journal of Computational Physics*, 227(2):1286 – 1305, 2007.

[29] S. Dubinkina and J. Frank. Statistical relevance of vorticity conservation in the hamiltonian particle-mesh method. *Journal of Computational Physics*, 229(7):2634 – 2648, 2010.

[30] V. Zeitlin. Finite-mode analogues of 2D ideal hydrodynamics: Coadjoint orbits and local canonical structure. *Physica D*, 49(3):353–362, 1991.

[31] T. DelSole. A fundamental limitation of Markov models. *Journal of the Atmospheric Sciences*, 57:2158–2168, 2000.

[32] B. Leimkuhler, E. Noorizadeh, and O. Penrose. Comparing the efficiencies of stochastic isothermal molecular dynamics methods. *Journal of Statistical Physics*, 143(5):921–942, 2011.

[33] C. Leith. Climate response and fluctuation dissipation. *Journal of the Atmospheric Sciences*, 32:2022–2026, 1975.

[34] A. J. Majda, R. Abramov, and M. Grote. *Information Theory and Stochastics for Multiscale Nonlinear Systems*, volume 25 of *CRM Monogr. Series*. American Mathematical Society, 2005.

[35] A. J. Majda, B. Gershgorin, and Y. Yuan. Low-frequency climate response and fluctuation–dissipation theorems: Theory and practice. *Journal of the Atmospheric Sciences*, 67(4):1186–1201, 2012/04/05 2009.

[36] A. J. Majda and I. Timofeyev. Remarkable statistical behavior for truncated Burgers-Hopf dynamics.

Proceedings of the National Academy of Sciences, 97(23):12413–12417 (electronic), 2000.

[37] A. J. Majda and I. Timofeyev. Statistical mechanics for truncations of the Burgers-Hopf equation: a model for intrinsic stochastic behavior with scaling. *Milan Journal of Mathematics*, 70:39–96, 2002.

[38] A. R. Abramov, G. Kovačič, and A. J. Majda. Hamiltonian structure and statistically relevant conserved quantities for the truncated Burgers-Hopf equation. *Communications on Pure and Applied Mathematics*, 56(1):1–46, 2003.

[39] W. E and J. C. Mattingly. Ergodicity for the Navier-Stokes equation with degenerate random forcing: Finite-dimensional approximation. *Communications in Pure and Applied Mathematics*, 54:1386–1402, 2001.

[40] P. J. Olver. *Applications of Lie groups to differential equations*, volume 107 of *Graduate Texts in Mathematics*. Springer-Verlag, New York, second edition, 1993.

[41] R. M. Miura, C. S. Gardner, and M. D. Kruskal. Korteweg-de Vries Equation and Generalizations. II. Existence of Conservation Laws and Constants of Motion. *Journal of Mathematical Physics*, 9:1204–1209, August 1968.

[42] R. McLachlan. Symplectic integration of Hamiltonian wave equations. *Numer. Math.*, 66(4):465–492, 1994.

[43] L. N. Trefethen. *Spectral Methods in Matlab*. Society for Industial and Applied Mathematics, 2000.